Research Square

Preprints are preliminary reports that have not undergone peer review.
They should not be considered conclusive, used to inform clinical practice,
or referenced by the media as validated information.

Sr–Nd isotopic systematics of archaeological ceramics from Central Europe: a methodological framework to study provenance and technology

Yulia Erban Kočergina
julie.erban@geology.cz
Czech Geological Survey
Tamara Sidorinová
Czech Geological Survey
Jaroslav Peška
ACO Archaeological Center Olomouc
Ondřej Pour
Czech Geological Survey
Jiří Frýda
Czech Geological Survey
Anna Vynnychuk
Czech Geological Survey

Article

Keywords: ceramics, pottery, strontium isotopes, neodymium isotopes, tracer, Central Europe

Posted Date: June 16th, 2026

DOI: https://doi.org/10.21203/rs.3.rs-9829345/v1

License: This work is licensed under a Creative Commons Attribution 4.0 International License.
Read Full License

Additional Declarations:
No competing interests reported.

Table 1, 2, and 3 are available in the Supplementary Files section.

Sr–Nd isotopic systematics of archaeological ceramics from Central Europe: a methodological framework to study provenance and technology

Yulia V. Erban Kochergina[1*], Tamara Sidorinová[1], Jaroslav Peška[2], Ondřej Pour[1], Jiří Frýda[1], Anna Vynnychuk[1]

[1]Czech Geological Survey, Klárov 3, 118 00 Prague, Czech Republic

[2]ACO Archaeological Center Olomouc, U Hradiska 42/6, 779 00 Olomouc, Czech Republic

[*]corresponding author

e-mail address: julie.erban@geology.cz

ORCID: 0000-0002-3938-8810

Key words: ceramics, pottery, strontium isotopes, neodymium isotopes, tracer, Central Europe

Highlights:

- Presents the first combined Sr–Nd isotopic dataset for archaeological ceramics from Central Europe (Neolithic to Early Middle Ages).
- Develops and tests a methodological framework for Sr–Nd isotope analysis of ceramic materials.
- Demonstrates contrasting behaviour of Nd and Sr isotopes during sampling, preparation, and post-depositional alteration.
- Shows the potential of combined Sr–Nd systematics for distinguishing local and regional ceramic production.
- Illustrates how isotopic data can be used to identify technological modification of ceramic raw materials.

ABSTRACT

Strontium and neodymium isotopes are powerful provenance tracers in geology, but their combined application to archaeological ceramics has so far been largely overlooked. This study presents the first integrated Sr–Nd isotopic dataset for archaeological ceramics from Central Europe, spanning the Neolithic to the Early Middle Ages, based on material from the long-occupied multi-cultural site at Přerov–Předmostí (Czech Republic). We develop and evaluate methods for ceramic sample preparation, chemical processing, and isotopic measurement using thermal ionisation mass spectrometry (TIMS), and assess potential sources of analytical and post-depositional modification.

Experimental results demonstrate that ceramics behave analogously to silicate rocks during digestion and isotope separation, permitting the application of standard geochemical protocols. Neodymium isotopes exhibit high internal homogeneity and low sensitivity to post-depositional alteration, whereas strontium isotopes show greater variability linked to vessel use, burial environment, and surface contamination. Combined Sr–Nd systematics enable discrimination between ceramics derived from contrasting geological settings and improve provenance resolution in loess-dominated landscapes. Application of the Přerov–Předmostí assemblage reveals the use of regionally sourced raw materials distinct from local daub clays and documents the technological modification of a Ca-rich ceramic paste in a Linear Pottery culture vessel. These results demonstrate the methodological potential of combined Sr–Nd isotope analysis for reconstructing ceramic raw material provenance, identifying production technologies, and tracing long-term patterns of resource exploitation.

1. INTRODUCTION

Isotopic ratio analysis has become an important tool in modern archaeology. Among radiogenic isotopes, strontium ($^{87}Sr/^{86}Sr$) has been most widely applied, while neodymium ($^{143}Nd/^{144}Nd$) has received very little attention. Strontium isotope analyses have utility in tracking past human migration and mobility (Adams et al., 2019; Bentley, 2006; Hodell et al., 2004; Perry et al., 2008; Schmidtová et al., 2026), animal mobility (Klontza-Jaklová et al., 2024) paleoecology (Stanley et al., 2003, Petrash et al., 2025), human diet (Dalle et al., 2022), wood provenances (Erban Kochergina et al., 2021, Rich et al., 2016, Vobejda et al, 2024, Imbert Štulc et al., 2023), pottery and glass production (Barfod et al., 2018; Carter et al., 2011; Degryse & Braekmans, 2014; Degryse & Schneider, 2008; Guzowska et al., 2003; Li et al., 2006), and metal artefacts (Felitsyn et al., 2019), rock artefacts (Christensen et al., 2006).

In contrast, archaeological studies rarely make use neodymium isotopes, even though they are a standard element in geological provenance research. Neodymium isotope analyses have been utilised to establish an isotope baseline for archaeological provenance in Silk Road regions (Lü et al., 2023) and to investigate the relationship between the Nd isotopic composition of human enamel and the geological area in which it was formed (Plomp et al., 2019). Sr and Nd isotopes could serve as effective tools for identifying local production and imports. Radiogenic isotope ratios ($^{87}Sr/^{86}Sr$, $^{143}Nd/^{144}Nd$) have also been utilised in ceramic analysis (De Bonis et al., 2018; Guzowska et al., 2003; Li et al., 2006).

In geochemistry, strontium and neodymium isotope systems are often used together because they provide complementary information. Strontium reflects the environmental calcium cycle and can vary even over short distances, while neodymium is closely bound to clay minerals and accurately records the geological background. Their combination therefore offers a powerful dual fingerprint: Sr provides sensitivity to local variations, and Nd adds robustness and long-term geological context.

Applying this dual approach to ceramics opens new possibilities for archaeology. By combining strontium and neodymium isotope data, we can more confidently distinguish local production from imports and reconstruct raw material sources with greater precision than with Sr alone.

Strontium is an alkaline earth element with an ionic radius similar to that of calcium (Ca). Accordingly, Sr^{2+} can substitute for Ca^{2+} in minerals such as Ca-feldspars, calcite, dolomite, and apatite, as well as in plant and animal tissues. It is almost omnipresent in nature, commonly in easily measurable amounts. Strontium has four stable isotopes: ^{84}Sr, ^{86}Sr, ^{87}Sr, and ^{88}Sr. While the proportions of ^{84}Sr, ^{86}Sr, and ^{88}Sr are nearly constant, the ^{87}Sr

content varies greatly because it is a daughter product of the radioactive decay of ^{87}Rb. The Sr isotopic composition is usually expressed as the $^{87}Sr/^{86}Sr$ ratio. As a rule of thumb, it can never be below 0.69899 (basaltic achondrite best initial BABI, Papanastassiou & Wasserburg, 1968). Values of $^{87}Sr/^{86}Sr$ between 0.702 and 0.707 are typical of mantle and mantle-derived lithologies (e.g., serpentinites, basalts). Marine sediments generally range from 0.707 to 0.709, while terrestrial sediments vary depending on their origin, usually between 0.705 and 0.750. Felsic rocks such as granites can cover the entire range, from 0.702 up to 1.0 or higher (Erban Kochergina et al., 2021; Faure & Mensing, 2005; Novak et al., 2025).

Rubidium is an alkali metal with a similar ionic radius to that of potassium. Rb^+ can substitute for K^+ in minerals such as K-feldspar and micas. Rubidium has two naturally occurring isotopes: the stable ^{85}Rb and the radioactive ^{87}Rb. The rubidium half-life of ^{87}Rb is 48.8 Byr (Steiger & Jager, 1977). Due to the long half-life of the $^{87}Rb \rightarrow {}^{87}Sr$ decay, the ^{87}Sr radiogenic ingrowth is very slow. The whole Sr isotopic system can thus be considered stable over the timescale of human history in most cases. In general, rocks or minerals with higher rubidium contents and of greater geological age yield higher present-day $^{87}Sr/^{86}Sr$ ratios when measured in the laboratory.

Samarium (Sm) and neodymium (Nd) are Rare Earth Elements (REE). Each has seven naturally occurring isotopes. The half-life of the $^{147}Sm \rightarrow {}^{144}Nd$ decay is approximately 106 billion years, more than double that of the Rb – Sr system. Like other REE, Sm and Nd exist in the trivalent (+3) state, forming relatively strong bonds (White, 2013). They are poorly soluble and only weakly mobile, even during weathering (Wilson, 2004). Because the half-life of the ^{147}Sm – ^{143}Nd system is extremely long, the variations in $^{143}Nd/^{144}Nd$ are very small, typically only in the third or fourth decimal place for most Earth materials. To facilitate interpretation, the epsilon (ε) notation is used, defined as $\varepsilon Nd = [(^{143}Nd/^{144}Nd)_{sample} / (^{143}Nd/^{144}Nd)_{CHUR} - 1] \times 10000$, where CHUR is Chondritic Uniform Reservoir (DePaolo &Wasserburg, 1976). The canonical CHUR value is $^{143}Nd/^{144}Nd=0.512638$ (Jacobsen & Wasserburg, 1980); however, in modern geochemical publications, the updated CHUR value of $^{143}Nd/^{144}Nd=0.512630$ proposed by Bouvier et al. (2008) is also used.

The use of epsilon value has two advantages: (1) the resulting variation is cast relative to a standard value – the isotopic composition of Bulk Earth; the so-called chondritic meteorites are a proxy for this; (2) because the slight variations in isotopic ratio are multiplied by 10000, the variation in most of Earth's reservoirs conveniently spans the range of +10 to –10 ε units.

Nd isotopic data are usually compared to CHUR calculated at the formation age of the rocks being studied, because whether a sample has positive ε (more radiogenic than CHUR) or negative ε (less radiogenic than

CHUR) conveys geological meaning. For archaeological samples, it is most practical to compare the measured Nd isotopic ratios directly with the present-day CHUR value (0.512638; Jacobsen & Wasserburg, 1980), without age-correction, since the geological age of the source material may vary widely.

The use of Sr and Nd isotopes as tracers relies on the fact that different natural reservoirs can display contrasting $^{87}Sr/^{86}Sr$ and $^{143}Nd/^{144}Nd$ isotopic signatures. These signatures mainly originate from rocks, which are the predominant source of Sr in nature. The isotopic signature of Sr and Nd in rocks results from the initial $^{87}Sr/^{86}Sr$ and $^{143}Nd/^{144}Nd$ ratios during their formation and the time-integrated ingrowth of radiogenic ^{87}Sr and ^{143}Nd since then. The effects of ingrowth are largest in samples with high parent/daughter (i.e., Rb/Sr or Sm/Nd) ratios. This results in distinct isotopic fingerprints of individual minerals, even within a single rock. Nd is relatively immobile in fluids and entirely immune to disturbances during low-temperature processes, such as erosion and sedimentation (Novák et al., 2025), and its isotopic composition can provide insights into the general provenance pattern. Firing ceramics at any temperature does not cause non-mass-dependent fractionation of radiogenic Sr and Nd isotopes; any mass-dependent fractionation, if present, is normalised away during data processing.

Therefore, we believe that the combined use of Sr and Nd isotopes can greatly contribute to determining the provenance of ceramics and to identifying imported ceramic goods.

This study aims to build on our previous work with geological samples and recent investigations of ceramics by establishing methods for preparing ceramic samples for Sr–Nd isotopic analyses and highlighting certain limitations in data interpretation. The objectives are therefore (i) to assess the suitability of Sr and Nd isotopes for determining the provenance of archaeological ceramics; (ii) to evaluate and improve sample preparation methods to reduce contamination and increase data reliability; and (iii) to explore the interpretative limitations of Sr–Nd isotope systematics within the context of ceramic provenance studies.

2. METHODS

2.1. Study site

The Přerov–Předmostí site (Central Moravia, Czech Republic) is situated on a loess terrace along the Bečva River at the edge of the Upper Morava Valley, near the Tršice Hills, within the Central Moravian Floodplain (Demek & Novák, 1992) (Fig.1). Its strategic location at the entrance of the Moravian Gate—a natural corridor linking the Pannonian Basin with the North European Plain—has made it a significant centre of human activity since the Palaeolithic (Klíma, 1990; Petřík et al., 2024). Archaeological research has uncovered a lengthy and

intricate settlement history, including the Linear Pottery culture (LBK), the Lengeyl culture (=Moravian Painted Pottery culture), Late Eneolithic and Bronze Age settlements and cemeteries, and La Tène and Medieval sites (Peška & Plaček, 2002; Petřík et al., 2024). Features and artefacts from excavations indicate multiple phases of occupation, particularly during the Neolithic and the beginning of the Eneolithic (Lengyel and Funnel Beaker cultures), Early Bronze Age (Nitra, Únětice, and Věteřov cultures), the Urnfield culture of the Late Bronze Age, and the Hallstatt and La Tène periods (Petřík et al., 2024). Important finds include Lengyel pits loaded with ceramics, Funnel Beaker ditches believed to be fortifications, Bell Beaker graves, and an Early Bronze Age fortified settlement at the southeastern boundary of Area 8. Artefacts such as a golden spiral (Urnfield culture), bone tools (Funnel Beaker culture), and a glass bracelet (La Tène period) exemplify the site's cultural diversity (Petřík et al., 2024). The geoarchaeological record of the gully fill reveals four major phases of settlement and erosion: the Early Bronze Age (2300 – 1600/1500 BC), the Young/Late Bronze Age (ca. 1500 – 900 BC), the Hallstatt period (900–400 BC), and the La Tène period (400 BC – 50 AD), each marked by cycles of intensive land use, deforestation, soil erosion, and colluvial deposition, alternating with intervals of relative stability and soil formation (Petřík et al., 2024).

2.2. Sample preparation and isotopic analyses

Sample preparation and geochemical analyses were performed at the Czech Geological Survey in Prague, Czech Republic.

2.2.1. Test archaeological samples

The initial objective was to assess the feasibility of conducting Sr – Nd isotope analyses on ceramic samples and to identify potential analytical complications. To this end, three ceramic specimens originating from the same locality Přerov–Předmostí but representing different chronological horizons were selected: sample 122 – ceramic belonging to the Urnfield culture (1300 – 750 BC); 142 – Bronze Age; 220 – Early Middle Ages. These samples were selected at random, solely to develop and practise the preparation procedure for Sr–Nd isotopic measurements. The analytical experience gained from processing these experimental specimens was subsequently applied to the preparation of the studied sample set. The experimental sherds were approximately 2–3 cm in diameter.

Microprobe analyses

At the beginning of our study, it was necessary to verify the homogeneity of the elemental concentrations throughout the entire thickness of the ceramic body. Therefore, epoxy pellets were prepared for electron microscopy. Elemental maps were generated, confirming the sample's elemental homogeneity (Fig. 2).

Maps of elemental distribution were performed by using a FEG-SEM Tescan MIRA 3GMU (housed at the Czech Geological Survey) equipped with two energy-dispersive spectrometers, Oxford Instruments Ultim Max 100. The maps were conducted with an accelerating voltage of 15 kV, absorbed current of ~3 nA, and working distance of 15 mm. The data was processed with Aztec 6.0 software (Oxford Instruments).

Sample preparation for measuring strontium and neodymium isotopic ratios

For test samples, it was necessary to verify the isotopic homogeneity across the sample. Therefore, each experimental sample was divided into three parts using a ceramic sherd: the outer part (o.), the inner part (i.), and the middle part (m.). We set the thicknesses of the outer and inner parts to 10–20% of the total thickness of the sherd. We ground the outer and inner samples with commercially available dental diamond drills. A separate drill bit was used for each sample. After grinding, we were left with approximately 70 – 80 % of the sample thickness, which we defined as the middle part of the sherd.

For preparation, Savillex® PFA vials were used to dissolve the sample, twice-distilled acids or ultra-pure acid in the case of hydrofluoric acid, using the methodology described in Erban Kochergina et al. (2022).

2.2.2. Studied samples

For this study, ceramic samples weighing at least 10 g were selected (Fig.3). To minimise possible contamination from either the period of use or the burial environment, the outer and inner layers of the sherds (approximately 10 – 15% of the sherd's thickness on each side) were removed. The sides of the sherds were also cut off where they had come into contact with the surrounding rock. The samples were then finely ground in an agate mill, and the resulting powder was used for chemical analysis. The pigment sample 5375 was carefully removed from the surface of the ceramic sherd 5374 with a scalpel.

For comparison, fragments of daub of different ages (samples 5594, 5595, and 5593), a local loess sample (5596), and an independent ceramic sample from a geologically distinct environment were included in the study. The strontium and neodymium isotopic compositions of these samples were analysed.

Determination of the elemental composition of ceramics using WD XRF

Concentrations of major (SiO_2, TiO_2, Al_2O_3, Fe_2O_3, MnO, MgO, CaO, K_2O, Na_2O, P_2O_5), trace elements (S, As, Ba, Bi, Cd, Co, Cr, Cu, Ge, Mo, Nb, Ni, Pb, Rb, Sn, Sr, Th, U, V, W, Zn, Zr) including rare earth elements (REE: La, Ce, Nd, Y) were analysed using X-ray fluorescence (XRF; Rigaku WD-XRF Primus 4). Samples (about 7 g) were prepared as pressed powder pellets without binders or other additives. Concentrations were determined using calibration-based methods. Replicate measurements of laboratory standards were used to monitor accuracy and precision, which were better than ± 5%. The detection limits of the Rigaku WD-XRF Primus 4 are presented in **Table 1**.

Sample digestion

About 0.2 g of powder was weighed, then dissolved in 7 ml of concentrated HF and 3 ml of concentrated HNO_3 at 140°C for 48 hours in Savillex PFA vials. The solution was evaporated to dryness. The residue was dissolved in 2 ml of the mixture of concentrated $HClO_4$ and 6M HCl (1:4) at 140°C for 12 hours and evaporated at 180°C. Then, three repeated dry-down steps were performed using 5 ml of concentrated HNO_3. The residue was completely dissolved in 4 ml of 6 M HCl.

Strontium and neodymium separation and measurement

Strontium and rare earth elements (REE) fractions were isolated from the bulk matrix by column chromatography techniques using a 4 ml column with AG-50W-X8 resin (Bio Rad, 200-400 mesh). The Sr resin from Triskem Intl. was used to further purify the Sr fraction (Erban Kochergina et al., 2022). The REE fraction was dried down with a mixture of H_2O_2 and 0.14M HNO_3 (1:10). The Nd was separated from the REE fraction with TRU-spec– Ln-spec resins (Erban Kochergina et al., 2022). Isotopic analyses of Sr and Nd were performed on a Thermo Fisher Triton Plus thermal ionisation mass spectrometer (TIMS) housed at CGS in static mode using a single Ta filament for Sr and static mode in a double Re filament assembly for Nd. The $^{143}Nd/^{144}Nd$ ratios were corrected for mass fractionation to $^{146}Nd/^{144}Nd = 0.7219$, $^{87}Sr/^{86}Sr$ ratios assuming $^{86}Sr/^{88}Sr = 0.1194$. The εNd values were obtained using Bulk Earth parameters of Jacobsen & Wasserburg (1980).

External reproducibility is estimated from repeat analyses of the JNdi-1 $^{143}Nd/^{144}Nd = 0.512100 \pm 07$, 2SM); NBS987: $^{87}Sr/^{86}Sr = 0.710259 \pm 14$, 2σ, n = 2. Basalt reference material BCR-2: $^{87}Sr/^{86}Sr = 0.705015 \pm 08$ (2SM), $^{143}Nd/^{144}Nd = 0.5126255 \pm 02$.

3. RESULTS

Test archaeological samples

The structure and texture of the samples are clearly visible in the BSE images (Fig. 2 a–c). These images were processed using graphic software to emphasise the pores, which are marked in red in figures 2 d–f. Samples 122 and 142 are characterised by larger mineral grains and a greater pore area compared to the fine-grained sample 220. Samples 122 and 142 contain quartz grains up to 1 mm in size (Fig. 2 g and h), whereas sample 220 contains quartz of a very fine grain size. Numerous cracks can be seen along the edges of the ceramic sherd in samples 142 (Fig. 2 e) and 220 (Fig. 2 f).

Elemental maps (Fig. 2 g–o, ESM_1) clearly show a uniform distribution of elements across the ceramic matrix. All samples have a similar mineral composition (ESM_2): quartz, K-feldspar, and apatite in sample 122, and biotite and muscovite in samples 142 and 220. Samples 122 and 220 contain small amounts of zircon (one to two grains per sample). Samples 122 and 142 have a comparable matrix composition (ESM_2), consisting of around 50 wt.% SiO_2, 19 – 25 wt.% Al_2O_3, and 5 – 16 wt.% Fe_2O_3.

The matrix of sample 220 contains 40 – 60 wt.% light elements that could not be identified by microprobe analysis. This sample also exhibits elevated phosphorus content (10 – 17 wt.% P_2O_5 on a 100% silicate basis, equivalent to 4 – 10 wt.% of the measured values). The Ca/P ratio in the matrix of sample 220 ranges from 0.9 to 1.2.

The Sr – Nd isotopic composition of the test samples is shown in Table 2. The Sr isotopic composition of the inner parts of the samples differs significantly from that of the middle and outer parts (Fig. 4).

The ε_{Nd0} of the three experimental samples ranges from -8 to -11, which is consistent with crustal rocks. There are also differences in the strontium (Sr) isotopic compositions ranging from 0.7119 to 0.7204 (Table 2).

Studied samples

Measured major and trace elements in the studied samples are listed in Table 3. At first glance, the samples seem to have a heterogeneous major-element composition: they contain between 44 and 71 wt.% SiO_2, 4 – 7 wt.% Fe_2O_3, and 14 – 17 wt.% Al_2O_3. The ternary diagram indicates that the elemental ratios are similar, with variations mainly due to differences in silica content. In terms of composition, the ceramic samples resemble pelites. Sample 5377 (LBK) is notably different, containing around 11 wt.% CaO compared to the other samples,

233 which contain only 1–3 wt.% (Table 3). Normalising trace element concentrations to the upper continental crust
234 yields values near unity, indicating that the studied ceramic samples have a composition similar to that of the
235 upper continental crust. The exceptions are P (roughly ten times higher) and Ba (about three times higher). As
236 illustrated in Fig. 5 a, all samples display a similar geochemical pattern, except for sample 5377, which exhibits
237 elevated concentrations of Sr, P, and Ba.

238 The Sr–Nd isotopic data for all studied samples are presented in Table 3 and illustrated in Fig. 8.

239 The nine ceramic samples from Přerov–Předmostí span a broad chronological range from the Neolithic to the
240 Early Middle Ages. Their $^{87}Sr/^{86}Sr$ ratios range from 0.7109 (sample 5377, LBK) to 0.7191 (sample 5381, Bell
241 Beaker culture), while εNd_0 values range from −8.8 (sample 5374, Lengyel culture) to −10.5 (sample 5381, Bell
242 Beaker culture). Despite spanning nearly five millennia, the majority of ceramic samples define a relatively
243 coherent isotopic field, with εNd_0 values clustering between −9.2 and −10.0 and $^{87}Sr/^{86}Sr$ ratios between 0.7148
244 and 0.7191, with the exception of sample 5377.

245 Sample 5377 (LBK, Neolithic) is clearly distinguished from the rest of the ceramic assemblage by its markedly
246 lower $^{87}Sr/^{86}Sr$ ratio (0.7109), while its εNd_0 value (−9.3) remains within the range of the other ceramics. This
247 decoupling of Sr and Nd isotopic signatures suggests a distinct raw material source or a specific technological
248 modification of the ceramic paste, rather than a fundamentally different clay provenance.

249 A notable isotopic contrast is observed between the ceramic sherd 5374 (Lengyel culture) and its associated
250 surface pigment 5375. The ceramic body yields $^{87}Sr/^{86}Sr = 0.7159$ and $\varepsilon Nd_0 = -8.8$, whereas the pigment shows
251 $^{87}Sr/^{86}Sr = 0.7139$ and $\varepsilon Nd_0 = -9.4$. Both the Sr and Nd isotopic compositions differ between the two materials,
252 indicating that the pigment was derived from a source isotopically distinct from the ceramic paste.

253 The three daub samples (5593, 5594, 5595), representing the LBK, Lengyel, and Únětice cultures, respectively,
254 are characterised by remarkably uniform Nd isotope compositions ($\varepsilon Nd_0 = -11.2$ in all three cases), suggesting
255 derivation from a common or isotopically homogeneous clay source repeatedly exploited over time. In contrast,
256 their $^{87}Sr/^{86}Sr$ ratios show greater variability, ranging from 0.7144 to 0.7175, which likely reflects within-profile
257 isotopic heterogeneity of a single loess-derived clay sequence or minor post-depositional Sr exchange.

258 Compared to the ceramic assemblage, the daub samples are systematically shifted towards lower εNd_0 values
259 (−11.2 versus −8.8 to −10.5).

The local loess sample (5596) yields $^{87}Sr/^{86}Sr = 0.7194$ and $\varepsilon Nd_0 = -10.9$. Its Nd isotopic composition is close to that of the daub samples, consistent with a common loess-derived provenance for daub clays. Its $^{87}Sr/^{86}Sr$ ratio is among the highest measured in this study, reflecting the typically more radiogenic Sr signature of loess deposits in this region (Waroszewski et al., 2021; Erban Kochergina et al., 2024).

The ceramic sample from the Celtic oppidum at Třísov (La Tène period) is isotopically distinct from all Přerov–Předmostí samples. It yields $^{87}Sr/^{86}Sr = 0.7232$ and $\varepsilon Nd_0 = -15.5$, placing it well outside the isotopic field defined by the Moravian assemblage.

4. DISCUSSION

4.1. How to prepare ceramic samples for Sr–Nd isotope analyses?

The behaviour of the analysed ceramic samples during decomposition, chemical separation, and isotopic measurement indicates that ceramics behave similarly to typical silicate rocks. This finding supports the use of standard silicate digestion and purification methods in ceramic isotope research.

Furthermore, our results show that when it is not possible to obtain a large amount of material for homogenisation, a small quantity (around 100 – 200 mg) of powder can be carefully scraped from the inner middle part of the ceramic body and used as a representative subsample for Sr–Nd isotopic analysis. The Nd isotopic composition seems to be uniform throughout the entire volume of the ceramic, indicating that neodymium isotopes are not significantly influenced by post-depositional processes or sample heterogeneity.

In contrast, the Sr isotopic composition might vary slightly due to external influences. This variation likely reflects interactions between the ceramic matrix and surrounding materials, such as soil or the burial substrate, as well as potential contamination from substances originally stored or processed in the vessel during its use. These findings emphasise the importance of careful sampling and awareness of potential Sr exchange processes when analysing strontium isotope data from archaeological ceramics.

Microscopic observations using a scanning electron microscope reveal that the outer regions of the ceramic fragments often display a higher density of microcracks (Fig. 2 d-f), which are more susceptible to contamination. This could explain the heterogeneity in the Sr isotopic composition observed across the ceramic sherds analysed in this study. However, the differences in isotopic composition between the outer and inner parts of the sherd (Table 2, Fig. 4) suggest the presence of two distinct types of contamination: (i) contamination that

occurred during the vessel's use, and (ii) contamination acquired during the burial period. Another finding of this study is that the pigment sample (5375) has a markedly different Sr–Nd isotopic composition compared to the ceramic sample (5374) to which it was applied: $^{87}Sr/^{86}Sr = 0.7139$, $\varepsilon Nd_0 = -9.4$ for the pigment and $^{87}Sr/^{86}Sr = 0.7159$, $\varepsilon Nd_0 = -8.8$ for the ceramic. Therefore, when preparing samples, it is important to remember that the increased porosity of the ceramic sherd or the presence of pigment on its surface may influence the resulting isotopic composition. As a result, we propose the procedure that we used in our study of the archaeological sample set from Přerov. This procedure involves carefully grinding off approximately 10 – 15% of the surface from both the inner and outer sides of the sherd. It also involves removing the lateral parts where the sherd was in contact with the burial environment.

When analysing coarse-grained ceramics, it is essential to determine whether the goal is to examine the bulk composition or to focus specifically on the ceramic body (matrix). If quartz grains were added to the ceramic paste as temper, this would influence the results of the major element analysis – the overall composition would show higher SiO_2 contents and, consequently, lower concentrations of other silicates, such as Al_2O_3 or Fe_2O_3 (see Table 1, Fig. 6).

Although quartz does not contain sufficient concentrations of Sr or Nd to significantly influence isotopic composition, its high abundance complicates sample dissolution. Dissolving large amounts of SiO_2 requires greater volumes of HF, increasing analytical costs and necessitating a larger sample mass to achieve sufficient signal intensity for Sr–Nd isotope measurements. For these reasons, we suggest removing large quartz grains prior to milling, as this facilitates subsequent preparation and isotope separation. If the sample was milled as a whole, including larger quartz grains, as was the case in the present study, this should be carefully considered when interpreting the data. Binary single-element diagrams should not be used; instead, ternary diagrams or binary ratio-ratio diagrams should be employed (Fig. 6).

4.2. Geochemical Approach to the Analysis of Archaeological Ceramics

Modern archaeological research offers a wide array of analytical methods for examining past human activities. In practice, the choice of method is often mainly dictated by a project's budget and the time required for laboratory analyses. Several petrographic and geochemical techniques used to study ceramics each offer specific advantages and limitations. Based on our experience with geological and archaeological materials, we propose the following workflow as a practical and reliable approach for preparing and conducting isotopic analysis of ancient ceramics (Fig. 7).

316 Before performing geochemical analyses, thorough archaeological documentation of the samples is crucial. The
317 samples selected for analysis should allow for the identification of their cultural context, the shape and size of
318 the vessel, and the location and conditions of their discovery. This information is essential for interpreting the
319 data. If any samples show a significantly different elemental or isotopic composition compared to the “local”
320 ceramics, it may indicate an imported product – in which case, a new archaeological investigation begins.

321 If analyses other than Sr – Nd isotope ratios are to be performed, we should choose one weighing at least 10 g.
322 (Fig. 7). Generally, the larger the mineral grains in a sample, the larger the sample size needed for analysis
323 (Kleeman, 1967). Conversely, the finer the ceramic fabric, the smaller the representative sample required. We
324 also need to account for grinding off 10 – 15% from each side of the fragment to remove any contamination. If
325 the sample contains large minerals, such as quartz, as temper, we must decide beforehand whether to measure
326 the entire sample or only the ceramic body. If choosing the latter, these large minerals should be removed before
327 grinding.

328 If possible, we suggest using a small portion of the sample to prepare thin sections or epoxy tablets for
329 microprobe analysis. These analyses will help us determine the mineral composition of the sample and establish
330 whether the material contains minerals that could be useful for geochronology. The U–Pb dating method for
331 zircon has been successfully employed in the study of pre-Hispanic ceramics from the La Morena site (Weber et
332 al. 2020), as well as in research on Maya pottery (Coffey et al. 2014), to identify their provenance. In our view,
333 the presence of larger amounts of zircon, along with the shape and size of its grains, can be a characteristic
334 feature of ceramic raw materials and assist in establishing their origin. We initially planned to separate zircon
335 grains because dating them using LA-ICP-MS could help determine the source of the clay raw material.
336 However, all analysed ceramic samples contained only 2 – 4 zircon grains, which are insufficient for this type of
337 analysis.

338 In the current project, the WD-XRF method was used for elemental analysis. High-pressure compressed pellets
339 were prepared without adding cellulose. During their preparation, careful attention was paid to purity and
340 reducing contamination, enabling the material to be suitable for future analyses. Here, the aim was to perform a
341 calibration analysis for the accurate determination of element concentrations.

342 An alternative to WD-XRF is traditional wet-chemical silicate analysis, combined with trace-element detection
343 by ICP-MS. The classical wet-silicate method allows the determination of both Fe^{2+} and Fe^{3+} concentrations, as
344 well as light elements such as Li and C. Typically, analysing these samples requires 5 – 10 g of material. Silicate

345 analysis, complemented by trace element assessment, especially REE using Q-ICP-MS, offers significant
346 interpretive flexibility. However, it should be noted that the cost is approximately twice that of WD-XRF. A
347 potential compromise involves analysing major elements by ICP-OES and trace elements by ICP-MS; however,
348 this approach remains more expensive than WD-XRF.

349 To determine Sr–Nd isotope ratios exclusively, approximately 100 mg of a representative sample is necessary.
350 When a rare artefact is unsuitable for destructive analysis, a precise spot on the sherd can be identified to
351 carefully remove a small amount of material. This process uses a pristine diamond drill bit, allowing for precise
352 extraction suitable for subsequent isotope and, if required, elemental analysis via ICP-MS.

353 If a larger amount of finely ground homogeneous ceramic sample is available, it is advised to dissolve at least
354 200 mg, with half of the solution being used for trace element analysis. The remaining half can then be utilised
355 to determine Sr and Nd isotope ratios.

356 *4.3. The Analytical Potential of Sr–Nd Isotopes in Ceramic and Glass Studies*

357 Although Sr and Nd isotope analysis of ceramics is still not widely applied, numerous studies have successfully
358 demonstrated its potential for glass provenance and technological reconstruction (Degryse & Schneider 2008;
359 Degryse et al., 2015; Gallo et al. 2015; Ganio et al., 2013; Henderson et al. 2015; Blomme et al. 2017). Isotopic
360 datasets have been used to identify groups of samples produced from similar raw materials and technological
361 recipes, to characterise glass production technologies, and to constrain the provenance of key raw materials. A
362 combined Sr–Nd approach has proven particularly powerful, as strontium isotopes mainly reflect the origin of
363 calcareous fluxes, whereas neodymium isotopes constrain the provenance of the siliceous component, allowing
364 technological and geological signals to be disentangled.

365 This approach has been applied across multiple chronological and regional contexts. For Roman glass, Sr–Nd
366 isotope systematics revealed dominant eastern Mediterranean raw material supply and enabled the identification
367 of multiple primary production centres (Degryse & Schneider, 2008; Blomme et al., 2017). Strontium isotope
368 ratios indicate that the calcium component was commonly derived from marine biogenic carbonates, such as
369 shell-rich coastal sands or deliberately added shell material, reflecting technological choices in flux selection,
370 whereas neodymium isotopes discriminate between eastern Mediterranean sources influenced by Nile-derived
371 sediments and more un-radiogenic western Mediterranean sands. Similar patterns were observed in northeastern
372 Italy, where most Roman and Late Roman glass was produced from coastal sands containing marine shells, with

Nd isotopes distinguishing between eastern and western Mediterranean raw material inputs and highlighting a stronger dominance of centrally produced eastern Mediterranean primary glass during the Late Roman period (Gallo et al., 2015). For Late Bronze Age glass, Sr – Nd isotopes clearly separate Mesopotamian and Egyptian production, reflecting the use of region-specific silica and flux sources (Degryse et al., 2015), while evidence from the Po Valley suggests the production of mixed-alkali glass from local raw materials and its subsequent mixing with potassium-rich glass derived from wood ash or halophytic plant ash linked to the Roman Magmatic Province (Henderson et al., 2015; Conticelli et al., 2002).

More recent applications further demonstrate the robustness of this method. Sr–Nd isotope data allowed the identification of multiple Islamic glass production regions and the establishment of a regional isotopic baseline for raw materials across the eastern Mediterranean and Near East (Henderson et al., 2020). Neodymium isotopes distinguished between coastal Levantine sands, inland Syrian sources, and possible Central Asian inputs, while strontium isotopes again reflected marine carbonate-derived fluxes, documenting geographically diverse supply networks. In contrast, Sasanian glass groups show that compositional variability primarily reflects technological differences in plant ash flux preparation rather than changes in silica provenance, with Nd isotopes indicating largely common sand sources and Sr isotopes recording chemically distinct plant ash batches (Ganio et al., 2013). Together, these studies demonstrate that combined Sr – Nd isotope systematics provide a robust framework for reconstructing both technological practices and raw material provenance in ancient glass production.

4.4. Key research questions addressed using Sr and Nd isotope systematics

I. Identification of compositional groups and local versus non-local production

Together with trace elements, Sr–Nd isotopes can be used to discriminate ceramic assemblages with similar elemental and isotopic compositions in large datasets and to identify compositional groups reflecting common raw material sources and technological recipes. Where geological backgrounds differ, this approach enables robust differentiation between locally produced ceramics and imported goods.

Our Sr–Nd isotopic data reveal a pronounced difference between the dataset from Přerov–Předmostí (Central Moravia, Czech Republic) and the sample from the Celtic oppidum at Třísov (South Bohemia, Czech Republic) (Fig. 8a, Table 3). This pattern is consistent with the contrasting geological settings of the two sites. The basement of the Třísov oppidum is dominated by granulites characterised by radiogenic (high) $^{87}Sr/^{86}Sr_0$ and less

radiogenic (low) $^{143}Nd/^{144}Nd_0$ ratios (Janoušek et al. 1995, 2008, 2022), whereas Přerov is situated within a loess-dominated region, where less radiogenic $^{87}Sr/^{86}Sr$ and more radiogenic $^{143}Nd/^{144}Nd$ signatures are expected (Waroszewski et al., 2021; Erban Kochergina et al., 2024).

To constrain the local isotopic signal at Přerov–Předmostí, we analysed the fragments of daub, which were most likely produced from locally available clay. The three daub samples represent different cultural periods (LBK, Lengyel culture, and Únětice culture). All three exhibits indistinguishable Nd isotope compositions (εNd_0 = −11.2) but various $^{87}Sr/^{86}Sr$ ratios, which may reflect within-profile variability of a single loess sequence (Waroszewski et al., 2021; Erban Kochergina et al., 2024). The loess sample shows a more radiogenic Sr isotopic composition and a similar Nd isotopic signature to the daub (εNd = −10.9). Comparison of the ceramic samples from Přerov–Předmostí with the local references (daub and loess) indicates a small but systematic offset, suggesting that the pottery was produced from regional raw materials that differ from those exploited for daub manufacture (Fig. 8).

II. Constraints on the provenance of clay and temper end-members

To constrain the provenance of clay raw materials and temper components, isotopic characterisation of individual end-members is essential. When temper consists of lithic fragments or recycled ceramic material and these components can be physically separated, their independent analysis allows a more robust identification of raw material sources and significantly improves the reliability of provenance attribution.

Currently, only a limited number of Sr–Nd isotopic datasets are available for sedimentary materials from the Moravian region. Waroszewski et al. (2021) reported Sr–Nd isotope compositions of Sudetic loess, while Erban Kochergina et al. (2024) published Sr isotope data for loess from two localities in South Moravia. In contrast, substantially more isotopic data exist for igneous rocks (Hanžl et al., 2019; Janoušek et al., 2020; Janoušek et al., 2022), which may represent important source components for clay raw materials (Fig. 8b).

The isotopic composition of the studied ceramic samples differs from that of Sudetic loess (Waroszewski et al., 2021) and from rocks of the Brno Massif (Hanžl et al., 2019), which has been proposed as a potential source area for Moravian loess deposits (Lisá, 2004) (Fig. 8 b). Instead, the prehistoric pottery samples show isotopic signatures comparable to those of rocks from the Třebíč pluton (Janoušek et al., 2020). If the ceramics were produced from local loess, this suggests that the Třebíč pluton may represent a dominant source of the coarse

(>75 μm) detrital fraction in the Přerov loess, a hypothesis that requires further verification through targeted paleoenvironmental and sediment provenance studies.

III. Technology of ceramic paste preparation

Within the ceramic dataset, sample LBK 5377 is clearly distinguished by the lowest $^{87}Sr/^{86}Sr$ ratio (0.7109) and highest CaO content (up to 10.7 wt.%). Although this pattern could potentially indicate imported goods, it more plausibly reflects the exploitation of a distinct clay source and/or a specific technological modification during paste preparation. This interpretation is further supported by trace-element systematics (Fig. 5a). Overall, the trace element data for sample LBK 5377 broadly resembles those of the other studied ceramics, but exhibits pronounced enrichment in Sr (481 ppm), P (1.88 wt.%) and Ba (0.21 wt.%). The Ca/P molar ratio of sample LBK 5377 (3.14), together with elevated P_2O_5 concentrations, indicates the presence of a phosphate-rich component mixed with a carbonate-bearing clay matrix, consistent with the addition of bone-derived material combined with loess-derived calcareous input.

Neither bone ash alone nor mixtures of bone ash and plant ash can explain the elevated Sr concentrations observed in this sample. Human bone typically contains ~100 – 300 ppm Sr (Schmidtová et al., 2026; Smrčka 2005), omnivores ~150 – 400 ppm, and herbivores ~400–500 ppm Sr (Smrčka 2005), whereas ash derived from wood and leaves contains <20 ppm Sr (Brüntgen et al., 2025; Novák et al., 2020). Accordingly, no binary mixing between ceramic material and ash, even when assuming variable bone-to-plant ash proportions, can reproduce the combined Sr enrichment and isotopic composition of sample LBK 5377. This suggests that the vessel was produced from a locally available clay with a Nd isotope signature consistent with the regional background, but characterised by a substantially higher CaO content than the clays used for the other analysed ceramics.

Vanková et al. (2019) reported the elemental and Sr isotopic composition of Jurassic limestones. Near Štramberk, about 50 km from the studied site, Jurassic limestone is quarried. Smaller limestone outcrops are also found closer to the study location. These lithologies likely represent a regional calcium source for ceramic raw materials. However, the deliberate addition of limestone as temper seems less probable because, although Jurassic limestones are Sr-rich (1115–1223 ppm) and have unradiogenic Sr isotope ratios (~0.7033), they alone cannot explain the high Ba and P concentrations seen in sample LBK 5377. A more plausible scenario involves using clay naturally enriched with CaO, possibly from loess deposits whose carbonate came from weathered Jurassic Ca-, Sr-rich limestones with low $^{87}Sr/^{86}Sr$ ratios. This raw material may have been technologically modified by adding ash, which could account for the combined enrichment of Ca, Sr, P, and Ba, as well as the

unique isotopic signature of sample LBK 5377. A larger set of LBK ceramics, combined with local geological reference samples, could help better understand regional clay-processing techniques.

IV. Constraining the timing and duration of raw material exploitation

Our dataset allows the reconstruction of the duration and continuity of clay deposit exploitation by different cultural groups. The combined evidence from major and trace element geochemistry together with Sr and Nd isotopic data indicates that different clay sources were used for daub production and ceramic manufacture. At the Přerov–Předmostí site, the same clay deposits were likely exploited from the Neolithic through the Early Middle Ages. These deposits probably represent relatively large clay sources, which increases the potential for their identification and targeted sampling in future field investigations.

V. Quantification of technological mixing and raw material proportions

Once the provenance of individual raw material end-members is constrained, their relative contributions can be quantitatively estimated using mass balance and isotopic mixing models, as demonstrated in previous studies (De Bonis et al., 2018). However, this approach becomes more complex when ceramic paste is produced from more than three source materials or when the exploited clay deposit itself is isotopically heterogeneous. Additional technological processes may further modify the original isotopic signal. For example, carbonate leaching during clay processing or the intentional addition of mica-rich temper can substantially alter the Sr isotopic composition of the ceramic paste.

The incorporation of mica-rich temper strongly affects Sr isotope ratios while exerting only a minor influence on Nd isotopes, thereby providing a sensitive tracer of technological modification that is largely independent of the primary clay provenance. This decoupling of Sr and Nd isotope systematics highlights the importance of integrating technological considerations into isotopic provenance interpretations.

5. CONCLUSIONS

Combined Sr–Nd isotope analysis is applicable to archaeological ceramics using standard silicate geochemical protocols, as ceramics behave analogously to silicate rocks during digestion, chemical separation, and isotopic measurement. This study establishes a practical step-by-step methodological workflow for ceramic sample preparation, chemical processing, and Sr–Nd isotopic measurement, and demonstrates its application on the first

integrated Sr–Nd dataset from Central Europe, spanning the Neolithic to the Early Middle Ages at the multi-period site of Přerov–Předmostí.

Neodymium isotopes show high internal homogeneity and are relatively insensitive to post-depositional alteration, making them a robust provenance tracer. Strontium isotopes, by contrast, show greater susceptibility to modification related to vessel use, burial conditions, and the presence of surface pigments, underscoring the importance of careful sampling and the removal of outer layers prior to analysis. The proposed workflow explicitly addresses these contrasting behaviours and provides practical guidance for sampling strategy, temper removal, and contamination control.

Ceramics from Přerov–Předmostí exhibit a systematic isotopic offset relative to local reference materials (daub and loess), suggesting the use of regional rather than strictly local raw materials. Isotopic overlap with the Třebíč pluton points to a potential contribution of this unit to the coarse detrital fraction of local loess deposits. The geochemically distinct LBK sample 5377 — characterised by elevated CaO, Sr, P, and Ba and relatively low $^{87}Sr/^{86}Sr$ — is best explained by technological modification of Ca-rich ceramic paste, likely involving carbonate addition and ash, rather than the import of finished vessels.

Overall, Sr–Nd isotope systematics represent a robust approach for distinguishing local from non-local production, reconstructing clay and temper provenance, identifying technological modification during paste preparation, and tracing long-term continuity in raw material exploitation. The methodological workflow proposed here is transferable to other ceramic assemblages and analytical laboratories, providing a replicable framework for future studies. Quantitative mixing models remain challenging where isotopically heterogeneous sources and multi-component mixtures are involved, reinforcing the need to integrate isotopic data with petrographic and geochemical evidence. Wider application of this combined approach to other Central European assemblages has the potential to significantly advance our understanding of ceramic exchange networks and raw material procurement strategies in prehistoric and early historic Europe.

6. FUNDING

The Czech Science Foundation supported this work, grant no. 26-21936N to YEK.

7. ACKNOWLEDGEMENTS

. We thank John Hora and Peter McArdle for insightful discussions and consultations, and Jan John for providing the ceramic sample from the oppidum of Třísov. During the preparation of this manuscript, ChatGPT (OpenAI) and Claude (Anthropic) were used for spell-checking and for designing the graphical layout of Figure 7.

8. ARCHAEOLOGICAL PERMITS AND PERMISSIONS

All archaeological materials analysed in this study were collected, sampled, and analysed under the permissions and regulations of the relevant institutions and heritage authorities responsible for their curation and protection.

9. DATA AVAILABILITY

All data generated or analysed during this study are included in this published article and its supplementary information files

519 **REFERENCES**

520 Adams, S., Grün, R., McGahan, D., Zhao, J., Feng, Y., Nguyen, A., Willmes, M., Quaresimin, M., Lobsey, B.,
521 Collard, M., Westaway, M.C. (2019). A strontium isoscape of north-east Australia for human provenance and
522 repatriation. *Geoarchaeology*, 34, 231–251. https://doi.org/10.1002/gea.21728

523 Barfod, G.H., Freestone, I.C., Lichtenberger, A., Raja, R., Schwarzer, H., (2018). Geochemistry of Byzantine
524 and Early Islamic glass from Jerash, Jordan: Typology, recycling, and provenance. Geoarchaeology 33, 623–
525 640. https://doi.org/10.1002/gea.21684

526 Bentley, R.A. (2006). Strontium isotopes from the earth to the archaeological skeleton: a review. *Journal of*
527 *Archaeological Method and Theory*, 13(3), 135–187. https://doi.org/10.1007/s10816-006-9009-x

528 Blomme, A., Degryse, P., Dotsika, E., Ignatiadou, D., Longinelli, A., Silvestri, A., (2017). Provenance of
529 polychrome and colourless 8th–4th century BC glass from Pieria, Greece: A chemical and isotopic approach. J.
530 Archaeol. Sci. 78, 134–146. https://doi.org/10.1016/j.jas.2016.12.003

531 Bouvier, A., Vervoort, J.D., Patchett, P.J., (2008). The Lu–Hf and Sm–Nd isotopic composition of CHUR:
532 Constraints from unequilibrated chondrites and implications for the bulk composition of terrestrial planets. Earth
533 Planet. Sci. Lett. 273, 48–57. https://doi.org/10.1016/j.epsl.2008.06.010

534 Büntgen, U., Oulehle, F., Oppenheimer, C., Svoboda, J., Erban Kochergina, Y. V., Rybníček, M., et al. (2025).
535 Potential and limitations of strontium isotopic fingerprinting in wood. Geophysical Research Letters, 52,
536 e2025GL117556. https://doi.org/10.1029/2025GL117556

537 Carter, S.W., Wiegand, B., Mahood, G.A., Dudas, F.O., Wooden, J.L., Sullivan, A.P., Bowring, S.A., (2011).
538 Strontium isotopic evidence for prehistoric transport of gray-ware ceramic materials in the eastern Grand
539 Canyon region, USA. Geoarchaeology 26, 189–218. https://doi.org/10.1002/gea.20348

540 Christensen, A.-M., Holm, P.M., Schuessler, U., Petrasch, J., (2006). Indications of a major Neolithic trade
541 route? An archaeometric geochemical and Sr, Pb isotope study on amphibolitic raw material from present day
542 Europe. Appl. Geochemistry 21, 1635–1655. https://doi.org/10.1016/j.apgeochem.2006.07.009

543 Coffey, K.T., Schmitt, A.K., Ford, A., Spera, F.J., Christensen, C., Garrison, J., (2014). Volcanic ash provenance
544 from zircon dust with an application to Maya pottery. Geology 42, 595–598. https://doi.org/10.1130/G35376.1

545 Conticelli, S., D'Antonio, M., Pinarelli, L., Civetta, L., (2002). Source contamination and mantle heterogeneity
546 in the genesis of Italian potassic and ultrapotassic volcanic rocks: Sr–Nd–Pb isotope data from Roman Province
547 and Southern Tuscany. Mineral. Petrol. 74, 189–222. https://doi.org/10.1007/s007100200004

548 Dalle, S., Snoeck, C., Sengeløv, A., Salesse, K.A., Hlad, M., Annaert, R., Boonants, T., Boudin, M., Capuzzo,
549 G., Gerritzen, C.T., Goderis, S., Sabaux, C., Stamataki, E., Vercauteren, M., Veselka, B., Warmenbol, E. & De
550 Mulder, G. (2022). Strontium isotopes and concentrations in cremated bones suggest an increased salt
551 consumption in Gallo-Roman diet. *Scientific Reports*, 12, 9280. https://doi.org/10.1038/s41598-022-12880-4

552 De Bonis, A., Arienzo, I., D'Antonio, M., Franciosi, L., Germinario, C., Grifa, C., Guarino, V., Langella, A.,
553 Morra, V., (2018). Sr-Nd isotopic fingerprinting as a tool for ceramic provenance: Its application on raw
554 materials, ceramic replicas and ancient pottery. J. Archaeol. Sci. 94, 55–69.
555 https://doi.org/10.1016/j.jas.2018.04.002

556 Degryse, P. & Braekmans, D., (2014). Elemental and isotopic analysis of ancient ceramics and glass. In: Cerling,
557 T. (Ed.), Treatise on Geochemistry, Vol. 14. Elsevier, Amsterdam, pp. 191–207. https://doi.org/10.1016/B978-0-
558 08-095975-7.01215-8

559 Degryse, P., Lobo, L., Shortland, A., Vanhaecke, F., Blomme, A., Painter, J., Gimeno, D., Eremin, K., Greene,
560 J., Kirk, S., Walton, M., (2015). Isotopic investigation into the raw materials of Late Bronze Age glass making.
561 J. Archaeol. Sci. 62, 153–160. https://doi.org/10.1016/j.jas.2015.08.004

562 Degryse, P., Schneider, J., (2008). Pliny the Elder and Sr–Nd isotopes: tracing the provenance of raw materials
563 for Roman glass production. J. Archaeol. Sci. 35, 1993–2000. https://doi.org/10.1016/j.jas.2008.01.002

564 Demek, J., Novák, V. (Eds.), (1992). Vlastivěda moravská: Země a lid. Nová řada, svazek 1 — Neživá příroda.
565 Muzejní a vlastivědná společnost, Brno. (*in Czech*)

566 DePaolo, D.J., Wasserburg, G.J., (1976). Nd isotopic variations and petrogenetic models. Geophys. Res. Lett. 3,
567 249–252. https://doi.org/10.1029/GL003i005p00249

568 Erban Kochergina Y.V., Erban V., Hora J.M., (2022). Sample preparation and chromatographic separation for
569 Sr, Nd, and Pb isotope analysis in geological, environmental, and archaeological samples. J. Geosci. 67 (3): 273
570 – 285. DOI: http://doi.org/10.3190/jgeosci.357

Erban Kochergina, Y.V., Erban, V., Novák, M., Štěpanová, M., (2021). $^{87}Sr/^{86}Sr$ isotope ratios in trees as an archaeological tracer: Limitations of linking plant-biomass and bedrock Sr isotope signatures. J. Archaeol. Sci. 133, 105438. https://doi.org/10.1016/j.jas.2021.105438

Erban Kochergina, Y.V., Pavlousek, P., Sanda, M., Hora, J.M., (2024). $^{87}Sr/^{86}Sr$ isotopic composition of wine: uses and limitations. OENO One 58, 1–15. https://doi.org/10.20870/oeno-one.2024.58.2.7451

Faure, G., Mensing, T.M., (2005). Isotopes: Principles and Applications, 3rd ed. John Wiley & Sons, Hoboken, NJ. ISBN 978-0-471-38437-3

Felitsyn, S.B., Alfimova, N.A., Bogomolov, E., (2019). Nd and Sr isotopic composition of ancient iron-made artifacts and ores from northwest Russia. Geoarchaeology 34, 221–228. https://doi.org/10.1002/gea.21695

Gallo, F., Silvestri, A., Degryse, P., Ganio, M., Longinelli, A., Molin, G., (2015). Roman and late-Roman glass from north-eastern Italy: The isotopic perspective to provenance its raw materials. J. Archaeol. Sci. 62, 55–65. http://doi.org/10.1016/j.jas.2015.07.004

Ganio, M., Gulmini, M., Latruwe, K., Vanhaecke, F., Degryse, P., (2013). Sasanian glass from Veh Ardašīr investigated by strontium and neodymium isotopic analysis. J. Archaeol. Sci. 40, 4264–4270. https://doi.org/10.1016/j.jas.2013.06.018

Guzowska, M., Kuleff, I., Pernicka, E., Satır, M., (2003). On the origin of Coarse Wares of Troia VII., in: Wagner, G.A., Pernicka, E., Uerpmann, H.-P. (Eds.), Troia and the Troad, Natural Science in Archaeology. Springer Berlin Heidelberg, Berlin, Heidelberg, pp. 233–249.

Hanžl, P., Janoušek, V., Soejono, I., Buriánek, D., Svojtka, M., Hrdličková, K., Erban, V., Pin, C., (2019). The rise of the Brunovistulicum: age, geological, petrological and geochemical character of the Neoproterozoic magmatic rocks of the Central Basic Belt of the Brno Massif. Int. J. Earth Sci. 108, 1165–1199. https://doi.org/10.1007/s00531-019-01700-2

Hasterok, D., Gard, M., & Webb, J. (2018). On the radiogenic heat production of metamorphic, igneous, and sedimentary rocks. *Geoscience Frontiers*. 9, 1777−1794. https://doi.org/10.1016/j.gsf.2017.10.012

595 Henderson, J., Evans, J., Bellintani, P., Bietti-Sestieri, A.-M., (2015). Production, mixing and provenance of Late
596 Bronze Age mixed alkali glasses from northern Italy: an isotopic approach. J. Archaeol. Sci. 55, 1–8.
597 https://doi.org/10.1016/j.jas.2014.12.006

598 Henderson, J., Ma, H., Evans, J., (2020). Glass production for the Silk Road? Provenance and trade of Islamic
599 glasses using isotopic and chemical analyses in a geological context. J. Archaeol. Sci. 119, 105164.
600 https://doi.org/10.1016/j.jas.2020.105164

601 Hodell, D.A., Quinn, R.L., Brenner, M., Kamenov, G., (2004). Spatial variation of strontium isotopes ($^{87}Sr/^{86}Sr$)
602 in the Maya region: a tool for tracking ancient human migration. J. Archaeol. Sci. 31, 585–601.
603 https://doi.org/10.1016/j.jas.2003.10.009

604 Holub, F.V., Janoušek, V., (2003). Geochemical and Sr-Nd isotopic constraints on the genesis of ultrapotassic
605 plutonic rocks from the Moldanubian zone of the Bohemian Massif. J. Czech Geol. Soc. 48, 61–62.

606 Iordanidis, A., Garcia-Guinea, J., Karamitrou-Mentessidi, G., (2009) Analytical study of ancient pottery from the
607 archaeological site of Aiani, northern Greece. Mater. Charact, 60, 292–302,
608 https://doi.org/10.1016/j.matchar.2008.08.001.

609 Imbert Štulc, A., Poszwa, A., Ponton, S., Dupouey, J.-L., Bouchez, J., Bardin, J., Delarue, F., Coubray, S.,
610 Lemoine, M., Rose, C., Ruelle, J., Beuret, M., Nguyen Tu, T.T., Dufraisse, A., (2023). Multi-elemental and
611 Strontium-Neodymium Isotopic Signatures in Charred Wood: Potential for Wood Provenance Studies. Int. J.
612 Wood Cult. 3, 464–500. https://doi.org/10.1163/27723194-bja10019

613 Jacobsen, S.B., Wasserburg, G.J., (1980). Sm-Nd isotopic evolution of chondrites. Earth Planet. Sci. Lett. 50,
614 139–155. https://doi.org/10.1016/0012-821X(80)90125-9

615 Janoušek, V., Erban Kochergina, Y.V., Andronikov, A.V., Magna, T., Holub, F.V., Trubač, J., Svojtka, M.,
616 Čejková, B., Erban, V., Magna, T., (2022). Decoupling of Mg from Sr–Nd isotopic compositions in Variscan
617 subduction-related plutonic rocks from the Bohemian Massif: implications for mantle enrichment processes and
618 genesis of orogenic ultrapotassic magmatic rocks. Int. J. Earth Sci. 111, 1491–1518.
619 https://doi.org/10.1007/s00531-020-01872-2

620 Janoušek, V., Hanžl, P., Svojtka, M., Hora, J.M., Erban Kochergina, Y.V., Gadas, P., Holub, F.V., Gerdes, A.,
621 Verner, K., Hrdličková, K., Daly, J.S., Buriánek, D., (2020). Ultrapotassic magmatism in the heyday of the

622 Variscan Orogeny: the story of the Třebíč Pluton, the largest durbachitic body in the Bohemian Massif. Int. J.
623 Earth Sci. 109, 1767–1810. https://doi.org/10.1007/s00531-020-01872-2

624 Janoušek, V., Rogers, G., Bowes, D., (1995). Sr-Nd isotopic constraints on the petrogenesis of the Central
625 Bohemian Pluton, Czech Republic. Geol. Rundschau 84, 520–534. https://doi.org/10.1007/BF00284518

626 Janoušek, V., Vrána, S., Erban, V., Vokurka, K., Drábek, M., (2008). Metabasic rocks in the Varied Group of the
627 Moldanubian Zone, southern Bohemia – their petrology, geochemical character and possible petrogenesis. J.
628 Geosci. 53, 31–46. https://doi.org/10.3190/jgeosci.019

629 Kleeman, A.W., 1967, Sampling error in the chemicalanalysis of rocks: Journal of the Geological Society
630 ofAustralia, v. 14, p. 43–47

631 Klíma, B., (1990). Mammoth Hunters from Předmostí, 1st edition. Lovci mamutů z Předmostí, 1. vyd.
632 Academia, Praha. (in Czech).

633 Klontza-Jaklová, V., Smíšek, M., Erban Kochergina, Y.V., Nevěčná, R., Zůbek, A., Sedláčková, L., Kos, P.
634 (2024). Horses in the suburbs of a medieval city – a case study from Brno (Czech Republic). Anthropozoologica,
635 59(11), 155–181. https://doi.org/10.5252/anthropozoologica2024v59a11

636 Li, B.-P., Zhao, J.-X., Greig, A., Collerson, K.D., Feng, Y.-X., Sun, X.-M., Guo, M.-S., Zhuo, Z.-X., (2006).
637 Characterisation of Chinese Tang sancai from Gongxian and Yaozhou kilns using ICP-MS trace element and
638 TIMS Sr–Nd isotopic analysis. J. Archaeol. Sci. 33, 56–62. https://doi.org/10.1016/j.jas.2005.06.007

639 Lisá, L., (2004). Exoscopy of Moravian eolian sediments. Bull. Geosci. 79, 177–182.

640 Lü, Q.-Q., Chen, Y.-X., Henderson, J., Bayon, G., (2023). A large-scale Sr and Nd isotope baseline for
641 archaeological provenance in Silk Road regions and its application to plant-ash glass. J. Archaeol. Sci. 149,
642 105695. https://doi.org/10.1016/j.jas.2022.105695

643 Munsell Color, (2000). Munsell Soil Color Charts. GretagMacbeth, New Windsor, NY.

644 Novak, M., Erban Kochergina, Y.V., Holmden, C., Andronikov, A.V., Kachlik, V., Kotkova, J., Andronikova,
645 I.E., Kirchner, J.W., Hruška, J., Veselovsky, F., Laufek, F., Pour, O., Stepanova, M., Sebek, O., Paces, T.,
646 Grabmüllerova, T., Curik, J., Prechova, E., Antalova, E., Vanisova, I., Komarek, A., (2025). Changing isotope
647 compositions of Mg, Ca and Sr in bulk crystalline rocks toward the weathering front: Disentangling inputs of

geogenic base cations into ecosystems. Appl. Geochem. 193, 106577.
https://doi.org/10.1016/j.apgeochem.2025.106577

Novak, M., Holmden, C., Farkaš, J., Kram, P., Hruška, J., Čurík, J., Veselovský, F., Štěpánová, M., Kochergina, Y. V., Erban, V., Fottová, D., Šimeček, M., Bohdálková, L., Přechová, E., Voldřichová, P., & Černohous, V. (2020). Calcium and strontium isotope dynamics in three polluted forest ecosystems of the Czech Republic, Central Europe. *Chemical Geology*, 119472. https://doi.org/10.1016/j.chemgeo.2020.119472

Papanastassiou, D.A. & Wasserburg, G.J., (1968). Initial strontium isotopic abundances and the resolution of small time differences in the formation of planetary objects. Earth Planet. Sci. Lett. 5, 361–376. https://doi.org/10.1016/S0012-821X(68)80066-4

Perry, M.A., Coleman, D. & Delhopital, N. (2008). Mobility and exile at 2nd century A.D. Khirbet edh-Dharih: Strontium isotope analysis of human migration in western Jordan. *Geoarchaeology, 23*(4), 528–549. https://doi.org/10.1002/gea.20230

Peška, J., Plaček, M., (2002). Dědictví věků: nemovité archeologické památky Přerovska. Archeologický centrum Olomouc, Olomouc (in Czech).

Petrash, D.A., Roeser, P., Kříbek, B., Staudigel, P.T., Bernecker, M., Jačková, I., Čejková, B., Erban Kochergina, Y.V., Koubová, M., Křížová, Š., Knésl, I., Laufek, F., Böttcher, M.E., Della Porta, G. & Fiebig, J. (2025). Drivers of episodic carbonate cementation during the Miocene Climatic Optimum in a paleolake of the Eger Rift. *Geochimica et Cosmochimica Acta*, 407, 47–66. https://doi.org/10.1016/j.gca.2025.08.025

Petřík, J., Adameková, K., Prišťáková, M., Petr, L., Tencer, T., Novák, J., Vrána, J., Kalábek, M., Peška, J., Milo, P., (2024). Fluctuating nature of prehistoric settlement and land use preserved in sedimentary record of vanished gully. Catena 243, 108128. https://doi.org/10.1016/j.catena.2024.108128

Plomp, E., von Holstein, I.C.C., Koornneef, J.M., Smeets, R.J., Baart, J.A., Forouzanfar, T., Davies, G.R., (2019). Evaluation of neodymium isotope analysis of human dental enamel as a provenance indicator using 10^{13} Ω amplifiers (TIMS). Sci. Justice 59, 322–331. https://doi.org/10.1016/j.scijus.2019.02.001

Pashkova, G. V., Statkus, M. A., Mukhamedova, M. M., Finkelshtein, A. L., Abdrashitova, I. V., Belozerova, O. Y., Chubarov, V. M., Amosova, A. A., Maltsev, A. S., Demonterova, E. I., & Shergin, D. L. (2023). A Workflow for Uncertainty Assessment in Elemental Analysis of Archaeological Ceramics: A Case Study of

675 Neolithic Coarse Pottery from Eastern Siberia. Heritage, 6(5), 4434-4450.
676 https://doi.org/10.3390/heritage6050234

677 Rich, S., Manning, S.W., Degryse, P., Vanhaecke, F., Van Lerberghe, K., (2016). Provenancing East
678 Mediterranean cedar wood with the 87Sr/86Sr strontium isotope ratio. Archaeol. Anthropol. Sci. 8, 467–476.
679 https://doi.org/10.1007/s12520-015-0242-7

680 Schmidtová, D., Hukelova, Z., Pinar Gil, J., Vyskočilová, G., Erban Kochergina, Y., Čejková, B., Garbaras, A.,
681 Steinhof, A., Cieszyńska, W.K., Šedo, O., Hofmanova, Z., Manzelli, V., Mazzini, L., Klontza, V., Fernandes, R.,
682 (2026). Multi-proxy data from Imola (Northern Italy) reveal diverse trajectories in human lifeways following the
683 collapse of the Western Roman Empire. R. Soc. Open Sci. 13, 251686. https://doi.org/10.1098/rsos.251686

684 Smrčka, V., (2005). Trace Elements in Bone Tissue. Karolinum Press, Prague, 214 pp. ISBN 80-246-1033-7.

685 Stanley, J.-D., Krom, M.D., Cliff, R.A. & Woodward, J.C. (2003). Short contribution: Nile flow failure at the
686 end of the Old Kingdom, Egypt: Strontium isotopic and petrologic evidence. *Geoarchaeology*, 18(3), 395–402.
687 https://doi.org/10.1002/gea.10065

688 Stanley, J.-D., Krom, M.D., Cliff, R.A., Woodward, J.C., (2003). Nile flow failure at the end of the Old
689 Kingdom, Egypt. Geoarchaeology 18, 395–402. https://doi.org/10.1002/gea.10065

690 Steiger, R.H., Jäger, E., (1977). Subcommission on geochronology: Convention on the use of decay constants in
691 geo- and cosmochronology. Earth Planet. Sci. Lett. 36, 359–362. https://doi.org/10.1016/0012-821X(77)90060-7

692 Taylor,S. R., andS. M.McLennan (1995), The geochemical evolution of the continental crust, Rev. Geophys.,
693 33(2), 241–265, doi:10.1029/95RG00262

694 Vaňková, L., Elbra, T., Pruner, P., Vašíček, Z., Skupien, P., Reháková, D., Schnabl, P., Košťák, M., Švábenická,
695 L., Svobodová, A., Bubík, M., Mazuch, M., Čížková, K., Kdýr, Š., (2019). Integrated stratigraphy and
696 palaeoenvironment of the Berriasian peri-reefal limestones at Štramberk (Outer Western Carpathians, Czech
697 Republic). Palaeogeogr. Palaeoclimatol. Palaeoecol. 532, 109256. https://doi.org/10.1016/j.palaeo.2019.109256

698 Vobejda, L., Šálková, T., Erban Kochergina, Y.V., Altman, J., Rybníček, M., (2024). Insight into the changes of
699 European agriculture during the age of Baroque and enlightenment: Interdisciplinary survey of manor farmyard
700 Švamberk (Czech Republic). Heliyon 10, e40916. https://doi.org/10.1016/j.heliyon.2024.e40916

Waroszewski J., Pietranik A., Sprafke T., Kabała C., Frechen M., Jary Z., Kot A., Tsukamoto S., Meyer-Heintze S., Krawczyk M., Łabaz B., Schultz B., Erban Kochergina Y.V. (2021): Provenance and paleoenvironmental context of the Late Pleistocene thin aeolian silt mantles in south-west Poland – a widespread parent material for soils. *Catena* 204, 105377. https://doi.org/10.1016/j.catena.2021.105377

Weber, M., Valencia, V., Caballero, J., (2020). U-Pb dating of zircon: A sourcing method for pottery from La Morena archaeological site, north-west Colombia. Archaeometry 62, 233–247. https://doi.org/10.1111/arcm.12532

White, W.M., (2013). Geochemistry. Wiley-Blackwell, Chichester, 668 pp. ISBN 978-0-470-65668-6

Wilson, M.J., (2004). Weathering of the primary rock-forming minerals. Clay Miner. 39, 233–266. https://doi.org/10.1180/0009855043930133

Tables:

Table 1. Major and trace element composition of ancient pottery from Přerov-Předmostí.

Table 2. Strontium–neodymium isotopic composition of archaeological test samples.

Table 3. Sr–Nd isotopic compositions, Munsell colour codes (Munsel color (2000)), cultural affiliations of studied samples from Přerov–Předmostí, and a reference ceramic sample from the Celtic oppidum at Třísov.

Figures:

Figure 1. (a)The study area in the context of Central Europe. (b) Geological map of the region. (c) Detailed map indicating archaeological excavation sites in Přerov - Předmostí.

Figure 2. Back scattered electron (BSE) photos and multiple EDS maps for the test archaeological samples (122, 142, 220).

Figure 3. Drawings of the shapes of the studied vessels. A description of the vessels is presented in Table 3.

Figure 4. The Sr–Nd isotopic composition of test archaeological samples. The graph shows differences in the Sr isotopic composition of a ceramic sherd between its outer and inner parts.

Figure 5. Bulk continental crust- normalized (Taylor & McLennan, 1995) trace elements patterns for (a) studied ceramic samples, (b) our studied samples-green, published data: samples from Eastern Siberia-red (Pushkova et al., 2023), samples from northern Greece-black (Iordanidas et al., 2009). This diagram shows the differ in trace element composition between datasets from different geological localities.

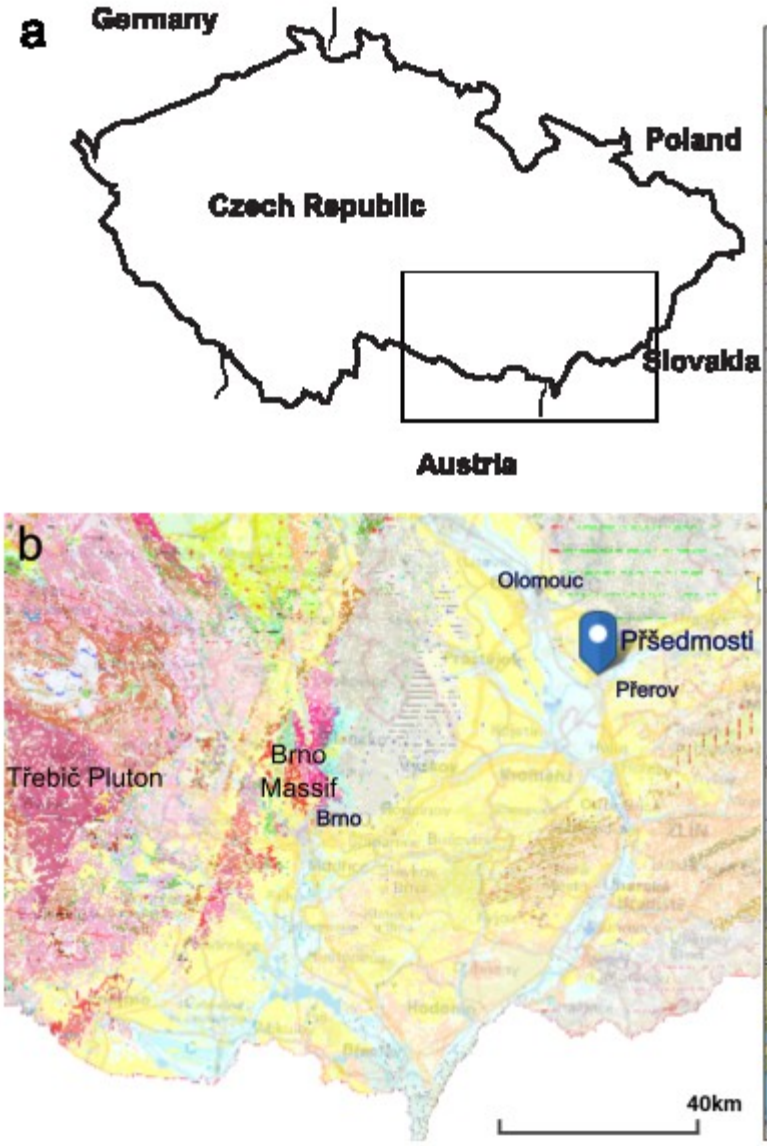
Figure 6. Ternary classification diagram $Al_2O_3+Fe_2O_3$ – SiO_2– CaO+MgO after Hasterok et al., (2018) for analyses of the Přerov-Předmostí ceramics.

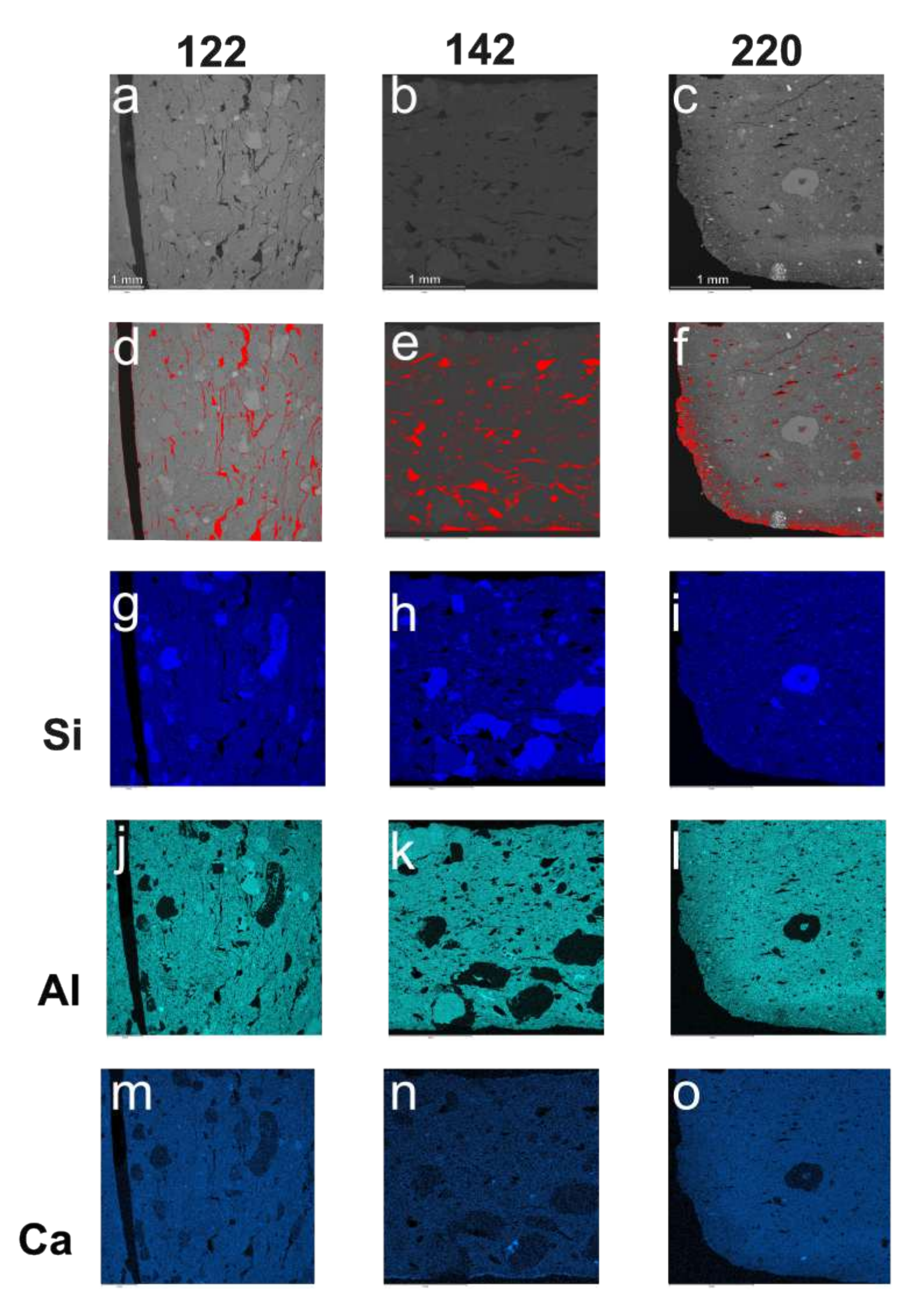
Figure 7. Methodological framework to study provenance and technology of archaeological ceramics. [1-] EPMA/SEM- Electron Probe MicroAnalysis/ scanning Electron Microscope. This methodology has significant potential; however, its applicability depends on the instrumentation available, particularly the presence of different detectors. In archaeological laboratories, instruments are primarily used for imaging (SEM), whereas geological laboratories more commonly employ EDS and WDS detectors, enabling more precise elemental analyses. [2-]Zircon ages determined by isotopic analyses are not useful for dating the artefact itself, however, the age spectrum can be indicative of the deposit used as a raw material, and therefore constrain provenance. [3-] In-situ isotope analyses are possible with laser ablation coupled with a collision reaction cell- equipped multi-collector ICP MS and have potential to dramatically decrease the amount of sample for analyses. [4-] Geochemical study of temper including isotopes can provide additional constrains on provenance and technology. Temper can be treated as a separate sample. [5-] if there is no contamination, the sample after XRD analysis can be used to determine the elemental composition. *- Pb for isotopic ratios determination could be separated together with Sr, the method described in Erban Kochergina et al., 2022.

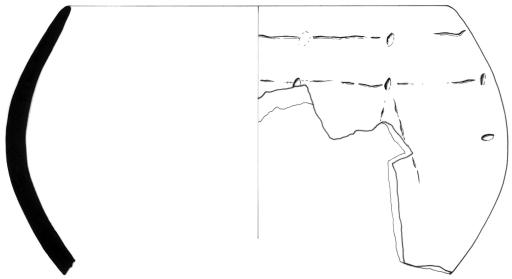
Figure 8. (a) Sr-Nd isotopic composition of Přerov-Předmostí ceramics and sample from the geologically distinct locality- oppidum Třísov. The Sr-Nd isotopic composition of the pigment (5375) differs from the Sr-Nd isotopic composition of the ceramic sample. The variability in $^{87}Sr/^{86}Sr$ coupled with uniformity in $^{143}Nd/^{144}Nd$ is indicative of Sr mobility contrasted with relative immobility of Nd. Therefor some portion of the Sr could have been replaced. (b) Sr-Nd isotopic composition of Přerov-Předmostí ceramics, which most likely correspond to local loess deposits, in comparison to possible source areas. The un-radiogenic Sr and CHUR-like Nd isotopic ratios of the Brno Massif preclude its involvement as a source to the Prerov ceramics. The inset shows a magnification of the remaining data, where the Prerov ceramics are isotopically more similar to the Třebic

753 Pluton (Janoušek et al., 2020; Holub & Janoušek, 2003) than to the Sudetic Loess (Waroszewski et al. 2021).

754 The scales between the two parts of the figure differ.

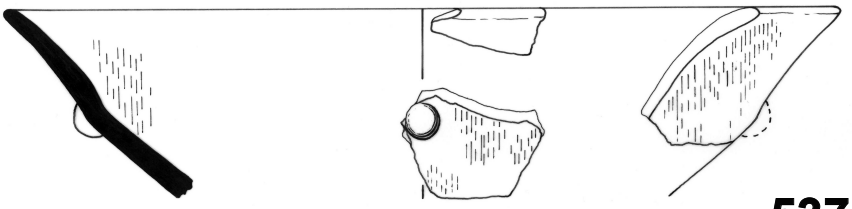

a
Germany
Poland
Czech Republic
Slovakia
Austria
b
Olomouc
Přšedmosti
Přerov
Brno
Massif
Brno
Třebič Pluton
40km
c
Předmosti 5
Předmosti 4
Předmosti 7
Předmosti 8
Předmosti 6
Dluhonice 2
850 m


122
142
220
a
b
c
1 mm
1 mm
1 mm
d
e
f
g
h
i
Si
j
k
l
Al
m
n
o
Ca



5377

PŘEROV - PŘEDMOSTÍ 6 | 16/2017 | OBJ. 54 | 16/2017-199-4

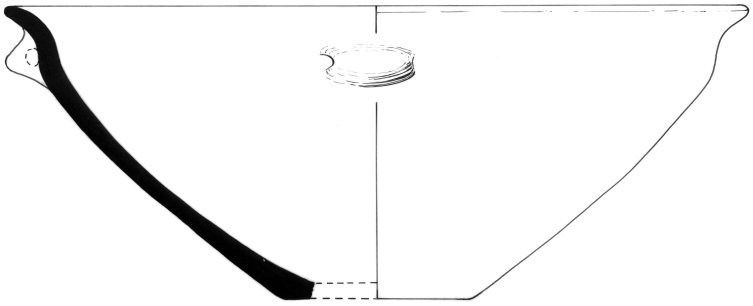


5374

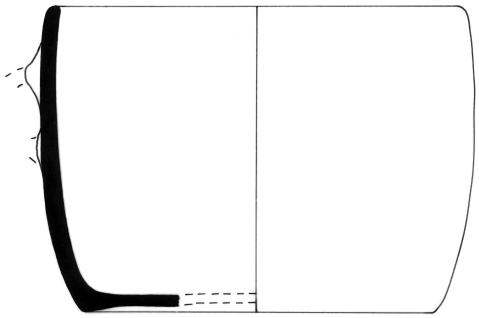
PŘEROV - MALÉ PŘEDMOSTÍ 7 | 20/2017 | OBJ. 166 | 20/2017-296-21

5375

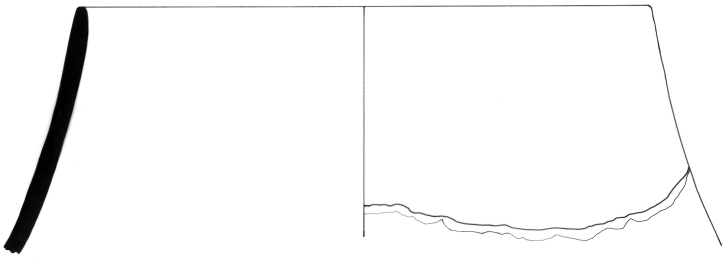
Red pigment



5381 PŘEROV - MALÉ PŘEDMOSTÍ 7 | 20/2017 | H 15 | 20/2017-826-2

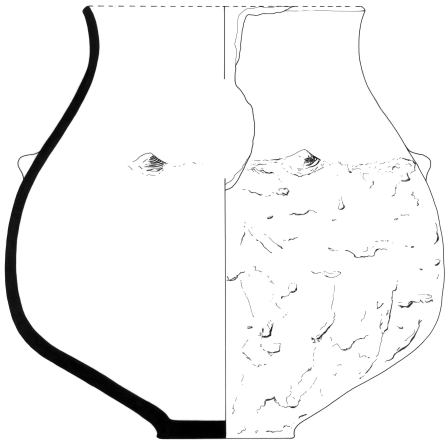


5380 PŘEROV - MALÉ PŘEDMOSTÍ 7 | 20/2017 | OBJ. 148 | 20/2017-290-1

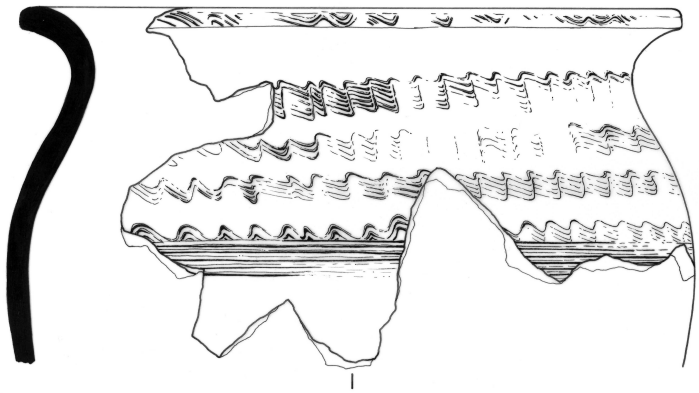


5379

PŘEROV - MALÉ PŘEDMOSTÍ 7 | 20/2017 | PLOCHA IX | ČTV. 13 | 20/2017-1363-53

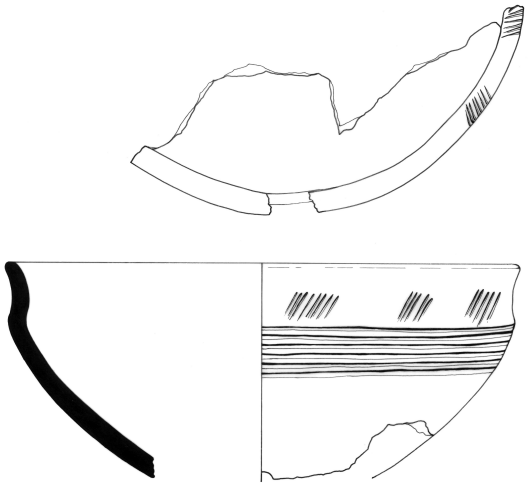


5378



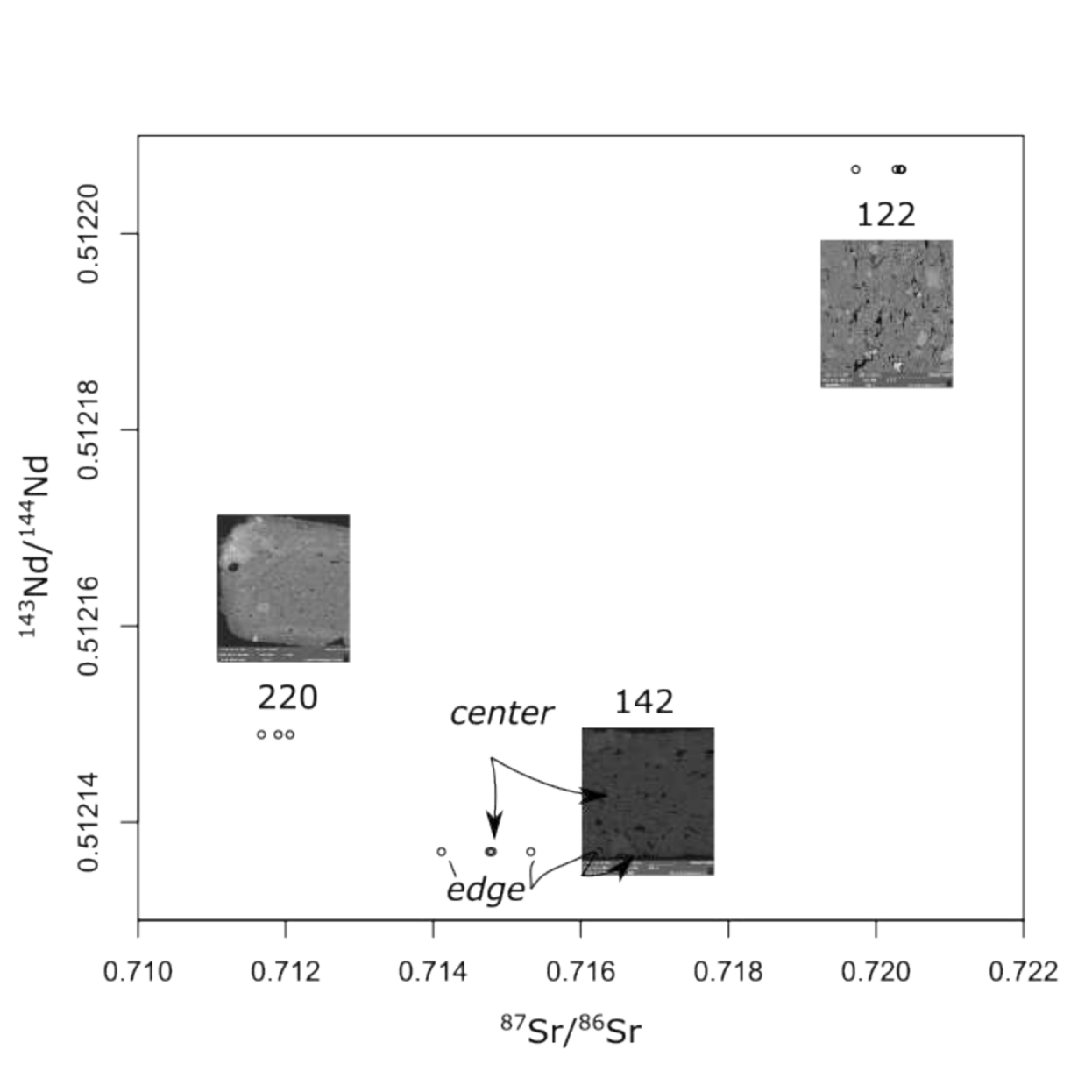
5382

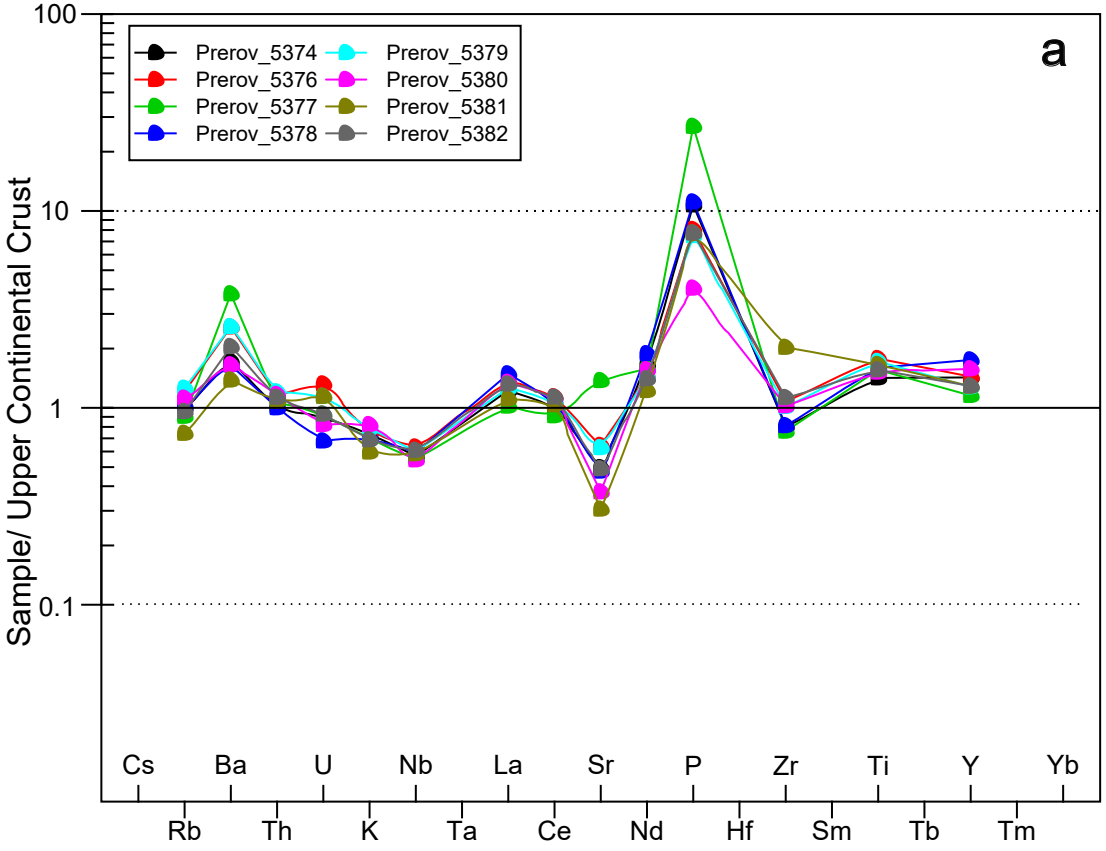
PŘEROV - MALÉ PŘEDMOSTÍ 7 | 20/2017 | OBJ. 657 | 20/2017-1471-6

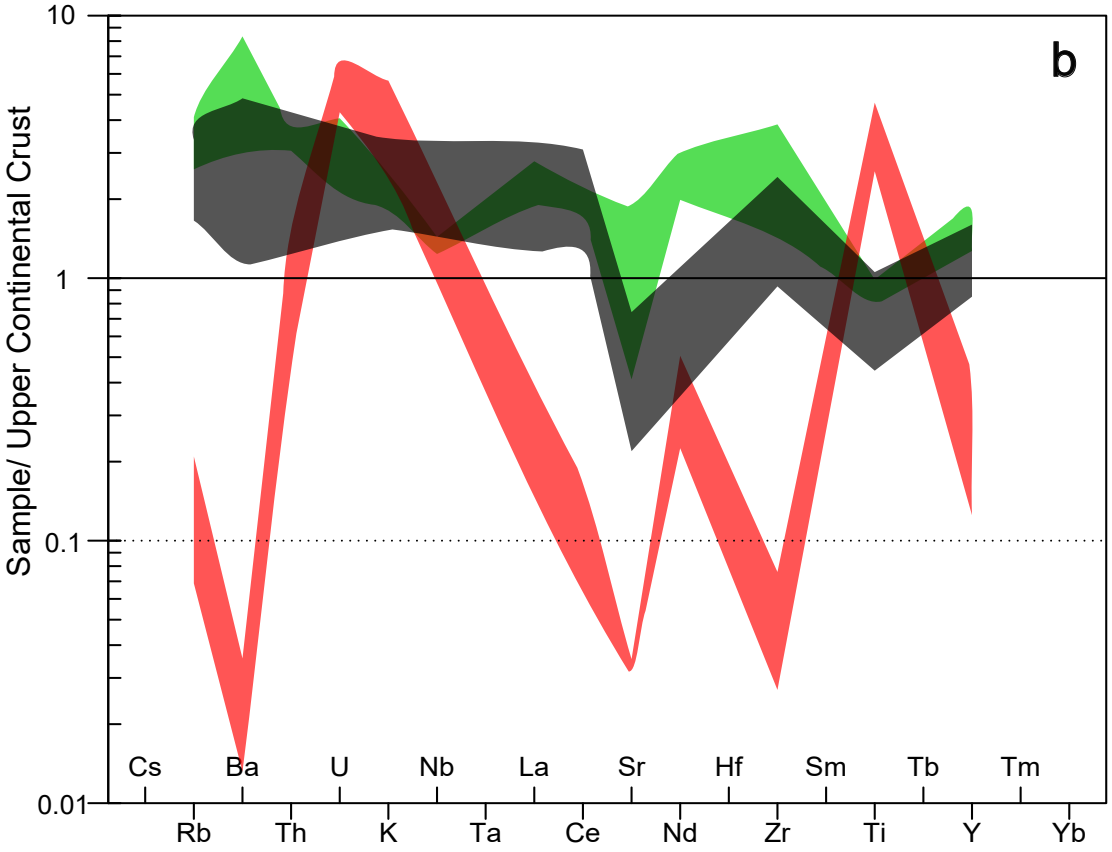


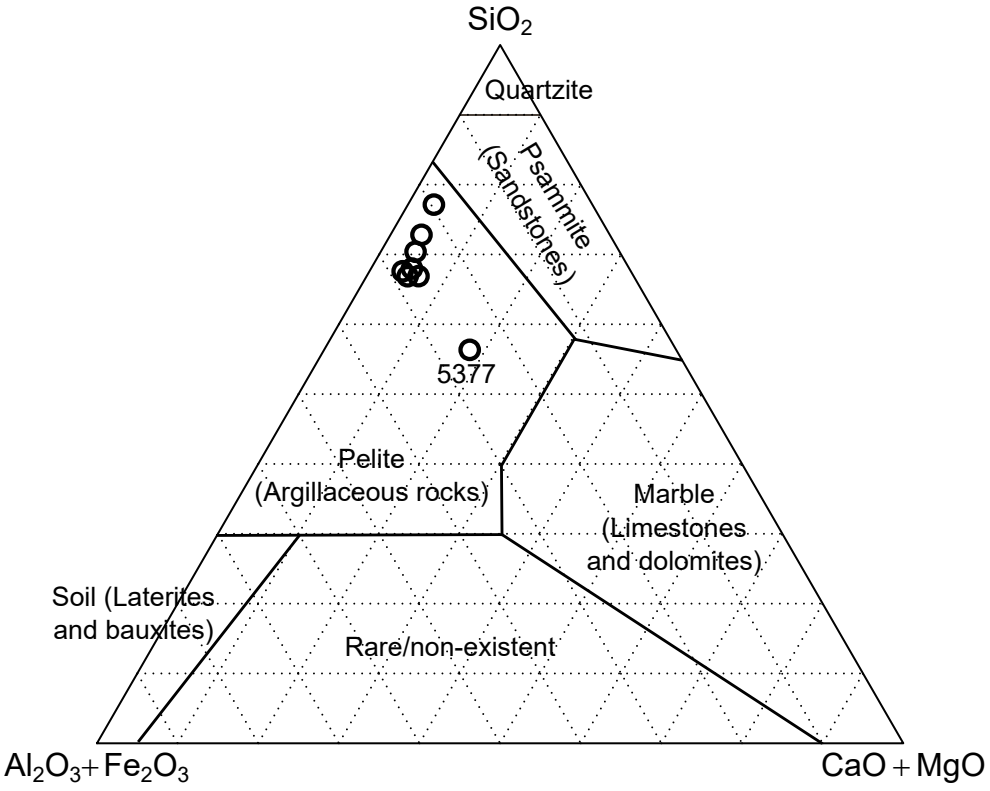
5376

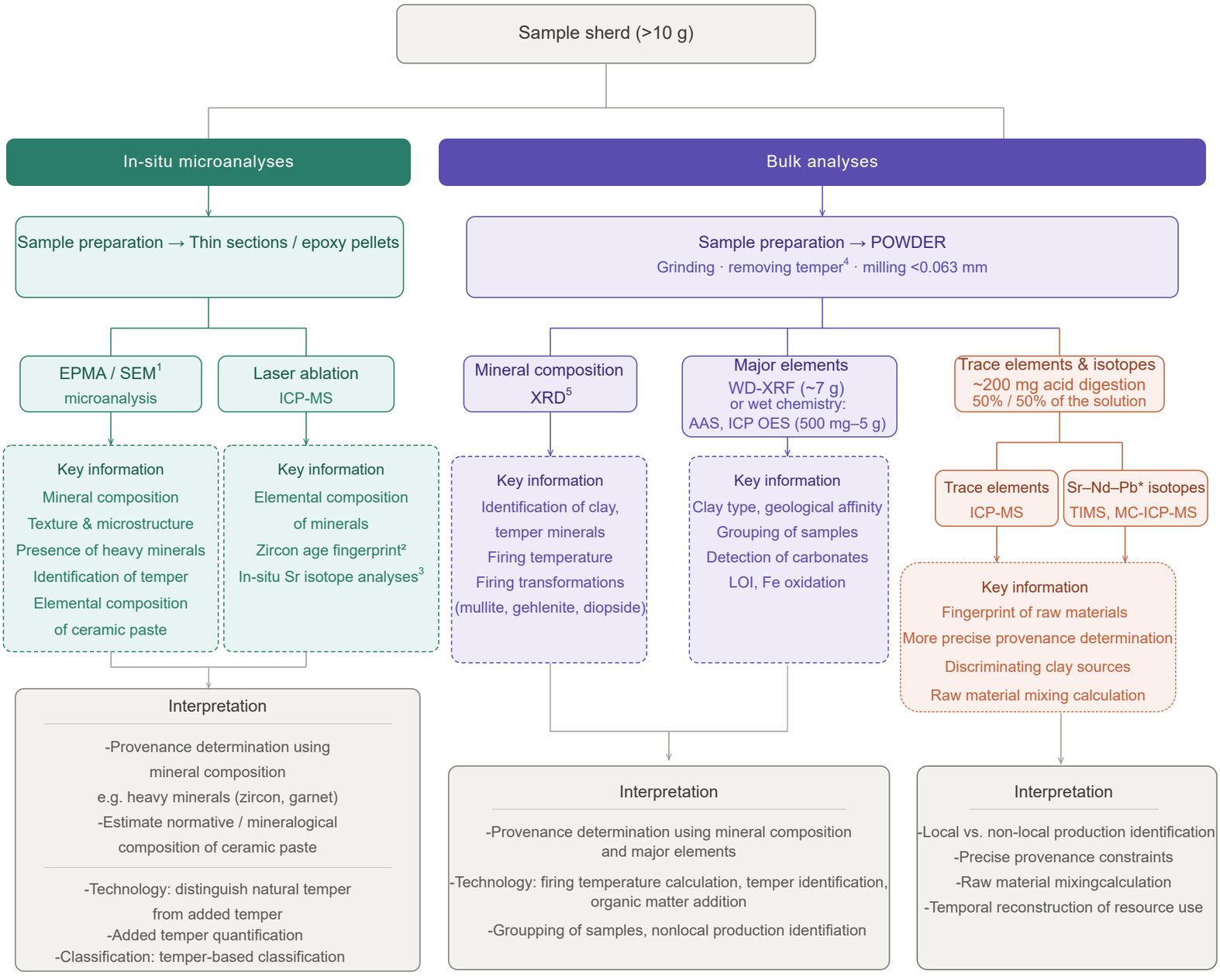
PŘEROV - MALÉ PŘEDMOSTÍ 7 | 20/2017 | PLOCHA VI | 20/2017-2276-1

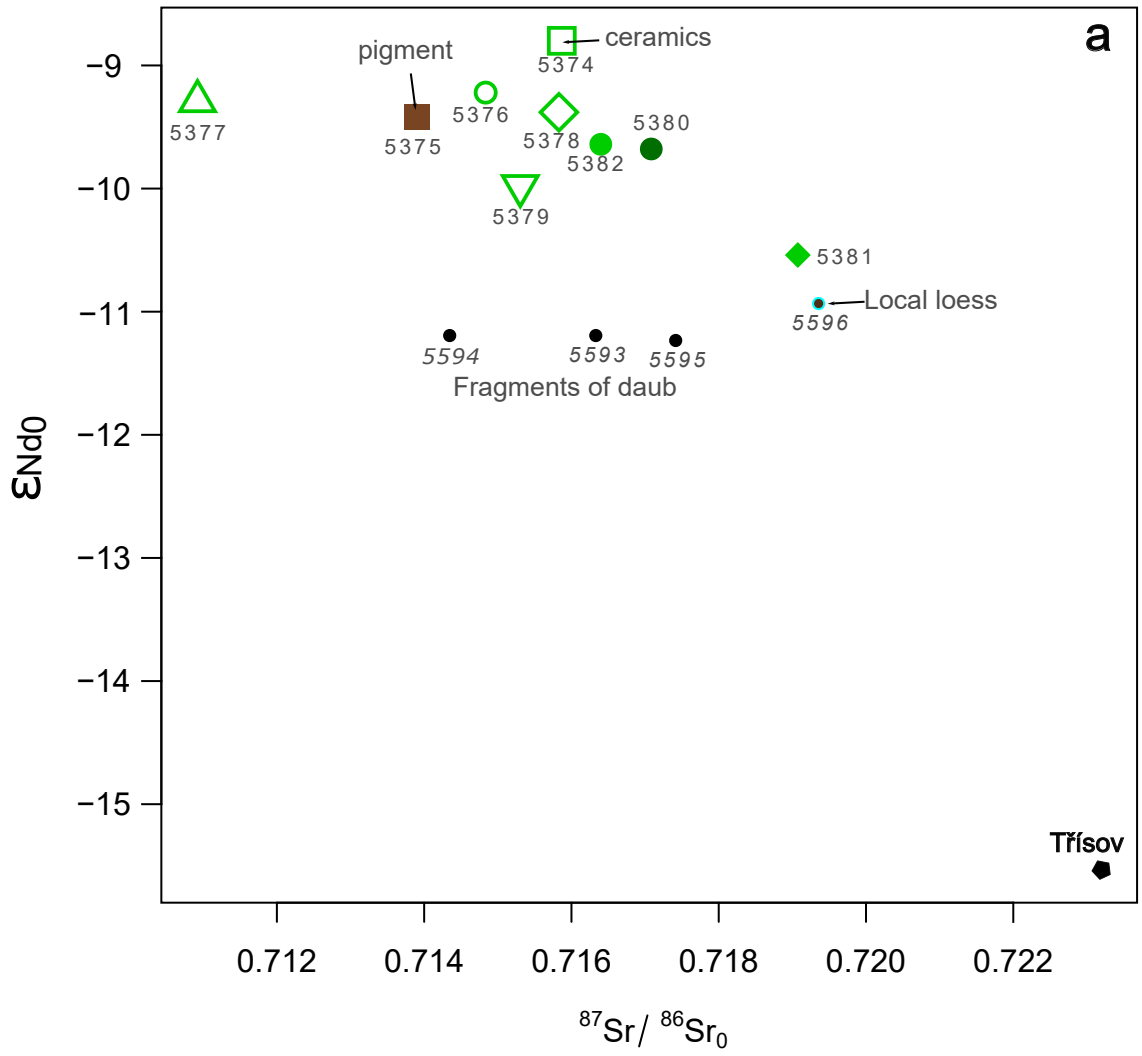

122
220
142
center
edge
0.51220
0.51218
0.51216
0.51214
$^{143}Nd/^{144}Nd$
0.710
0.712
0.714
0.716
0.718
0.720
0.722
$^{87}Sr/^{86}Sr$

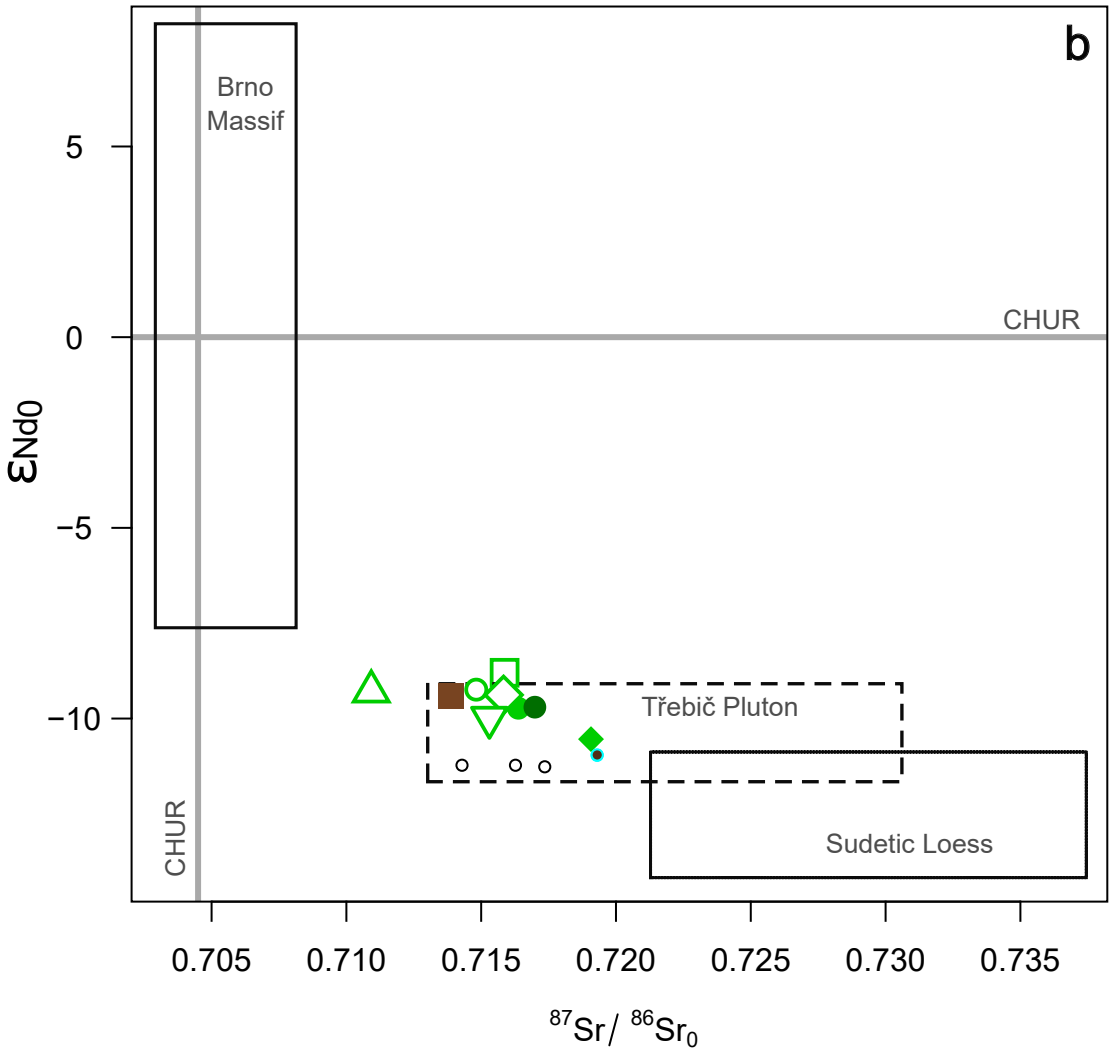

a
Prerov_5374
Prerov_5376
Prerov_5377
Prerov_5378
Prerov_5379
Prerov_5380
Prerov_5381
Prerov_5382
Sample/ Upper Continental Crust
100
10
1
0.1
Cs
Rb
Ba
Th
U
K
Nb
Ta
La
Ce
Sr
Nd
P
Hf
Zr
Sm
Ti
Tb
Y
Tm
Yb


b
Sample/ Upper Continental Crust
10
1
0.1
0.01
Cs
Rb
Ba
Th
U
K
Nb
Ta
La
Ce
Sr
Nd
Hf
Zr
Sm
Ti
Tb
Y
Tm
Yb


SiO_2
Quartzite
Psammite
(Sandstones)
5377
Pelite
(Argillaceous rocks)
Marble
(Limestones
and dolomites)
Soil (Laterites
and bauxites)
Rare/non-existent
$Al_2O_3 + Fe_2O_3$
$CaO + MgO$


Sample sherd (>10 g)
In-situ microanalyses
Bulk analyses
Sample preparation → Thin sections / epoxy pellets
Sample preparation → POWDER
Grinding · removing temper[4] · milling <0.063 mm
EPMA / SEM[1]
microanalysis
Laser ablation
ICP-MS
Mineral composition
XRD[5]
Major elements
WD-XRF (~7 g)
or wet chemistry:
AAS, ICP OES (500 mg–5 g)
Trace elements & isotopes
~200 mg acid digestion
50% / 50% of the solution
Key information
Mineral composition
Texture & microstructure
Presence of heavy minerals
Identification of temper
Elemental composition
of ceramic paste
Key information
Elemental composition
of minerals
Zircon age fingerprint²
In-situ Sr isotope analyses[3]
Key information
Identification of clay,
temper minerals
Firing temperature
Firing transformations
(mullite, gehlenite, diopside)
Key information
Clay type, geological affinity
Grouping of samples
Detection of carbonates
LOI, Fe oxidation
Trace elements
ICP-MS
Sr–Nd–Pb* isotopes
TIMS, MC-ICP-MS
Key information
Fingerprint of raw materials
More precise provenance determination
Discriminating clay sources
Raw material mixing calculation
Interpretation
-Provenance determination using
mineral composition
e.g. heavy minerals (zircon, garnet)
-Estimate normative / mineralogical
composition of ceramic paste
-Technology: distinguish natural temper
from added temper
-Added temper quantification
-Classification: temper-based classification
Interpretation
-Provenance determination using mineral composition
and major elements
-Technology: firing temperature calculation, temper identification,
organic matter addition
-Groupping of samples, nonlocal production identifiation
Interpretation
-Local vs. non-local production identification
-Precise provenance constraints
-Raw material mixingcalculation
-Temporal reconstruction of resource use


a
pigment
ceramics
5374
5377
5376
5375
5378
5380
5382
5379
5381
Local loess
5596
5594
5593
5595
Fragments of daub
Třísov
−9
−10
−11
−12
−13
−14
−15
εNd0
0.712
0.714
0.716
0.718
0.720
0.722
87Sr/ 86Sr0


b
Brno
Massif
CHUR
Třebič Pluton
Sudetic Loess
CHUR
5
0
−5
−10
εNd0
0.705
0.710
0.715
0.720
0.725
0.730
0.735
87Sr/ 86Sr0

Supplementary Files

This is a list of supplementary files associated with this preprint. Click to download.

- ErbanKocherginaetal.Table1.xlsx
- ErbanKocherginaetal.Table2.xlsx
- ErbanKocherginaetal.Table3.xlsx
- esm1.pdf
- ESM2table.xlsx